

UC Berkeley

SEMM Reports Series

Title

Ritz Method for Dynamic Analysis of Large Discrete Linear Systems With Non-Proportional Damping

Permalink

<https://escholarship.org/uc/item/7b94p2t9>

Authors

Ibrahimbegovic, Adnan

Chen, Harn-Ching

Wilson, Edward

et al.

Publication Date

1989-07-01

**REPORT NO.
UCB/SEMM 89/15**

**STRUCTURAL ENGINEERING,
MECHANICS AND MATERIALS**

**RITZ METHOD FOR DYNAMIC ANALYSIS
OF LARGE DISCRETE LINEAR SYSTEMS
WITH NON-PROPORTIONAL DAMPING**

By:

ADNAN IBRAHIMBEGOVIC, HARN C. CHEN,

EDWARD L. WILSON and ROBERT L. TAYLOR

JULY 1989

**DEPARTMENT OF CIVIL ENGINEERING
UNIVERSITY OF CALIFORNIA
BERKELEY, CALIFORNIA**

RITZ METHOD FOR DYNAMIC ANALYSIS OF LARGE DISCRETE LINEAR SYSTEMS WITH NON-PROPORTIONAL DAMPING

A. Ibrahimbegovic, H. C. Chen, E. L. Wilson and R. L. Taylor

Department of Civil Engineering
University of California, Berkeley, CA 94720, U.S.A.

1. INTRODUCTION

The dynamic analysis of practical engineering structures requires the solution of a large system of dynamic equilibrium equations. For the loading of short duration (impulse loading) step-by-step numerical procedures are usually the most effective. However, for the loading of long duration, such as earthquake, mode superposition procedure is the appropriate numerical method (see Wilson [1977]).

Traditional mode superposition procedure requires the solution of the eigenvalue problem as the first step. Once eigenpairs are known, modal transformation that utilizes only a small portion of the complete spectrum will usually yield a very good approximation to the exact dynamic response. To improve the approximation properties of the eigenvector basis employed in modal transformation, the procedures of static correction and mode acceleration are used in order to account for the contribution of higher truncated modes.

An alternative approach to ensuring good approximation properties of vector basis used for modal transformation is the use of the Ritz procedure. We want to emphasize the difference between the Ritz method on one side versus the Rayleigh-Ritz and the Lanczos method on the other side. While the later two methods consider the eigenvalue problem solution, the Ritz method (see Ritz [1909]) considers the possibilities for the *approximate* solution of partial differential equations (e.g. the equations that govern the motion of deformable body) as a series solution of *admissible* functions. For the discrete system (or the set of semidiscrete equations), we are confined to, a set of admissible vectors (further referred as *Ritz vectors*) is easy to construct. An additional benefit of the Ritz method is that the eigenvalue problem does not have to be solved. However, the numerical technique used to generate Ritz vectors will strongly influence the quality of results obtained. The load dependent vector algorithm, first proposed by Wilson et al. [1982], combines the advantages of the Rayleigh-Ritz procedure and the static correction method.

Analogy of recurrence equations for generating vector basis with Lanczos process for computing eigenvalues (see Lanczos [1950] or Parlett [1980]), provides satisfying Rayleigh-Ritz approximation properties to the true eigenvectors, while the choice of starting vector, as a static response to fixed loading form, provides the benefits of static correction concept.

For the structural systems where a reasonable degree of homogeneity in the energy loss mechanism exists, damping is modeled as proportional or classical. The general representation of proportional damping is first given by Caughey [1960] in the series form proportional to powers of mass and stiffness matrix. Rayleigh damping is included into the series as a linear combination of mass and stiffness proportional terms. As an alternative to the series form of Caughey [1960], a proportional damping matrix can be obtained directly from specified modal damping ratio values as shown by Wilson and Penzien [1972].

However, for the problems where large differences in energy dissipation mechanisms exist, assumption on proportional damping is not realistic. Some examples of the linear dynamic systems with non-proportional damping are mechanical systems with special energy absorbing devices and coupled systems for analysis of soil-structure and fluid-structure interaction. Several possibilities (see Clough and Mohtajedi [1976]) exist to treat non-proportionally damped dynamic linear systems by mode superposition procedure within the framework of real eigenvector basis. A rigorous procedure to devise the coordinates that uncouple equations of motion utilizes complex vector basis for modal transformation first given by Foss [1958].

Recent research (see Wilson et al. [1982], Nour and Clough [1984] and Leger and Wilson [1987]) indicated the superiority of the load dependent vector algorithm in generating Ritz vector basis for mode superposition in the case of proportional damping. The Krylov subspace (commonly used name in mathematics community for the vector sequence generated in the process) can be spanned by Lanczos vectors as in Nour and Clough [1984] (which furnish tridiagonal modal stiffness form), or alternatively, by Ritz vector basis as in Wilson et al. [1982] (which yields diagonal form for both modal stiffness and mass matrix). Motivated by those results we propose the analogous approach to dynamic analysis of linear systems with non-proportional damping.

Two procedures for generating real and complex vector basis by the load dependent vector algorithm are compared in this study. The real vector basis is generated by the load dependent vector algorithm with selective orthogonalization (see Ibrahimbegovic and Wilson [1989]), and numerical integration of modal equations coupled by velocity proportional forces is performed by an efficient iterative procedure as described in Ibrahimbegovic and Wilson [1988]. The complex vector basis is generated by the load dependent vector algorithm as described in Chen and Taylor [1988], applied to the adequate first order form of the equations of motion. Both procedures are reviewed in sections 3 and 4, after some considerations of their common characteristics are given in section 2. In section 5 we present a comparison of two vector basis, real and complex, for the two typical examples of

structures characterized by non-proportional damping : flexible mechanical system with concentrated dampers and soil-structure interaction problem which arises in analysis of dam-foundation system. In section 6 we give some closing remarks.

2. RITZ METHOD FOR DISCRETE SYSTEMS

The standard form of the semidiscrete equations of motion that describe how small displacements from equilibrium evolve in time is

$$\mathbf{M} \ddot{\mathbf{u}}(t) + \mathbf{C} \dot{\mathbf{u}}(t) + \mathbf{K} \mathbf{u}(t) = \mathbf{f}(t) \quad (2.1)$$

where \mathbf{M}, \mathbf{C} and \mathbf{K} are, respectively, the $n \times n$ mass, damping and stiffness matrices, while $\ddot{\mathbf{u}}(t)$, $\dot{\mathbf{u}}(t)$ and $\mathbf{u}(t)$ are $n \times 1$ acceleration, velocity and displacement vectors.

In many practical analysis of complex dynamic systems, the sheer size of the problem turns the exact solution to (2.1) into prohibitively expensive computational effort. Therefore, an approximate solution is often sought. One way to obtain an approximate solution to (2.1) leads to the Ritz method, in which a series form is assumed

$$\mathbf{u}(t) = \sum_{i=1}^m \boldsymbol{\phi}_i y_i(t) = \boldsymbol{\Phi} \mathbf{y}(t) \quad (2.2)$$

Since normally $m < n$, this approach can be interpreted as a process of *projection* of the original *space* $\mathbf{u}(t) = (u_1(t), \dots, u_n(t))$ to the *subspace* $\mathbf{y}(t) = (y_1(t), \dots, y_m(t))$. The set of projection vectors $\boldsymbol{\Phi} = (\boldsymbol{\phi}_1, \dots, \boldsymbol{\phi}_m)$, or the *subspace vector basis*, has to be admissible in accordance to the Ritz method. If $\boldsymbol{\Phi}$ is the set of eigenvectors of the system (2.1), the traditional mode superposition method is recovered.

By utilizing transformation (2.2) into (2.1), a new set of equations of motion can be written in terms of generalized *Ritz coordinates*

$$\mathbf{M}_m \ddot{\mathbf{y}}(t) + \mathbf{C}_m \dot{\mathbf{y}}(t) + \mathbf{K}_m \mathbf{y}(t) = \mathbf{f}_m(t) \quad (2.3)$$

where

$$\mathbf{M}_m = \boldsymbol{\Phi}^T \mathbf{M} \boldsymbol{\Phi} \quad (2.4)$$

$$\mathbf{C}_m = \boldsymbol{\Phi}^T \mathbf{C} \boldsymbol{\Phi} \quad (2.5)$$

$$\mathbf{K}_m = \boldsymbol{\Phi}^T \mathbf{K} \boldsymbol{\Phi} \quad (2.6)$$

$$\mathbf{f}_m(t) = \boldsymbol{\Phi}^T \mathbf{f}(t) \quad (2.7)$$

Beside the reduction in size (from n to m), additional benefit of (2.3) versus (2.1) is possibly gained in the *uncoupled* form of equations of motion. For \mathbf{M} , \mathbf{C} and \mathbf{K} being real, symmetric and positive definite matrices, it is always possible (see Parlett [1980]) to choose a set of *eigenvectors* $\boldsymbol{\Phi}$ which yields the diagonal form in (2.3) for two of them. The traditional approach, with an important physical

interpretation, is to diagonalize \mathbf{M} and \mathbf{K} , i.e.

$$\mathbf{M}_m = \mathbf{I} = \text{diag}(1, \dots, 1) \quad (2.8)$$

and

$$\mathbf{K}_m = \Omega_m^2 = \text{diag}(\omega_1^2, \dots, \omega_m^2) \quad (2.9)$$

If the matrix \mathbf{C} shares the same set of eigenvectors as \mathbf{M} and \mathbf{K} , then (2.3) reduces to *uncoupled* set of equations. This is more general condition on the form of \mathbf{C} that uncouples the equations of motion than the Caughey series (Caughey [1960]).

By utilizing spectral decomposition theorem (see Parlett [1980]) the *proportional* damping matrix \mathbf{C} can be presented as a *summation* of *rank-one* matrices

$$\mathbf{C} = \sum_{i=1}^n \lambda_C \phi_i \phi_i^T \quad (2.10)$$

However, the main interest of our study is associated with the case when the damping matrix \mathbf{C} is not of the form (2.10), i.e. we deal with *non-proportional* damping.

3. REAL VECTOR BASIS

In this section we give a short review of the load dependent vector algorithm used for generation of the real vector basis. For more extensive discussion we refer to previous work by Wilson et al. [1982], Nour and Clough [1984] and Ibrahimbegovic and Wilson [1989]. A simple and efficient procedure, described previously in Ibrahimbegovic and Wilson [1988], is then used to solve modal equations of motion coupled only by velocity proportional forces.

The real Ritz vector basis is generated for the system (2.1) disregarding the nature of dissipative term. Namely, the equations of motion we start with are

$$\mathbf{M} \ddot{\mathbf{u}}(t) + \mathbf{K} \mathbf{u}(t) = \mathbf{f}(t) = \sum_{i=1}^l \mathbf{f}_i g_i(t) \quad (3.1)$$

The loading of special form separable in time and space is required for successful use of load dependent vector algorithm. For many applications (e.g. earthquake loading) series representation of loading in (3.1) contains one term only. For simplicity let us proceed with those cases.

The starting vector in the subspace generation is chosen as a static response to constant spatial distribution of loading

$$\mathbf{r}_1 = \mathbf{K}^{-1} \mathbf{f} \quad (3.2)$$

$$\beta_1^2 = (\mathbf{r}_1^T \mathbf{M} \mathbf{r}_1)^{1/2} \quad (3.3)$$

$$\mathbf{q}_1 = \mathbf{r}_1 / \beta_1 \quad (3.4)$$

The choice of the starting vector in (3.2) is motivated by the *static correction* concept (see Maddox [1975]), which accounts for the contribution of truncated modes in the approximate static manner. The starting vector is then the static response normalized (3.4) with respect to mass weighted inner product (3.3).

Other vectors are generated by the recurrence equation that employs *dynamic matrix* $\mathbf{K}^{-1} \mathbf{M}$ (see Clough and Penzien [1975]), i.e.

$$\bar{\mathbf{r}}_{j+1} = \mathbf{K}^{-1} \mathbf{M} \mathbf{q}_j \quad (3.5)$$

The dynamic matrix is self-adjoint with respect to mass weighted inner product, i.e. for any two vectors \mathbf{q}_i and \mathbf{q}_j it holds

$$(\mathbf{q}_i, \mathbf{K}^{-1} \mathbf{M} \mathbf{q}_j)_{\mathbf{M}} = \mathbf{q}_i^T \mathbf{M} \mathbf{K}^{-1} \mathbf{M} \mathbf{q}_j = (\mathbf{q}_j, \mathbf{K}^{-1} \mathbf{M} \mathbf{q}_i)_{\mathbf{M}} \quad (3.6)$$

The sequence of vectors is thus orthonormalized with respect to mass matrix by utilizing the Gram-Schmidt procedure.

A typical three-term recurrence equation that will generate real vector basis for use in modal transformation is :

$$\beta_{j+1} \mathbf{q}_{j+1} = \mathbf{r}_{j+1} = \mathbf{K}^{-1} \mathbf{M} \mathbf{q}_j - \alpha_j \mathbf{q}_j + \beta_j \mathbf{q}_{j-1} \quad (3.7)$$

where

$$\alpha_j = \mathbf{q}_j^T \mathbf{M} \mathbf{K}^{-1} \mathbf{M} \mathbf{q}_j \quad (3.8)$$

and

$$\beta_j = \mathbf{q}_{j-1}^T \mathbf{M} \mathbf{K}^{-1} \mathbf{M} \mathbf{q}_j \quad (3.9)$$

as an alternative formula to compute β_j .

The recurrence equations (3.7) are equivalent to the ones in Lanczos algorithm (see Parlett [1980] or Nour and Clough [1984]). This analogy provides the load dependent vector algorithm with a good Rayleigh-Ritz approximation for the fundamental eigenvalues of the system. Beside the special choice of the starting vector, this is the major reason for the exceptional performance of the load dependent vector algorithm. The analogy can be also utilized in defining the selective orthogonalization strategy (see Parlett [1980]). The selective orthogonalization strategy requires monitoring the convergence of Ritz values to eigenvalues at each step; hence, for the short runs full reorthogonalization (see Wilson et al. [1982]) is usually insignificant increase of the computational effort. Finally, the analogy was utilized to define the new spectral content truncation criteria in the process of vector basis generation, that account for the different range of dominant exciting frequency (see Ibrahimbegovic and Wilson [1989]).

After m steps of the process tridiagonal matrix T_m is generated

$$T_m = Q^T M K^{-1} M Q = \begin{bmatrix} \alpha_1 & \beta_2 & & & & \\ \beta_2 & \alpha_2 & \beta_3 & & & \\ & & \ddots & \ddots & & \\ & & & \ddots & \ddots & \\ & & & & \beta_{m-1} & \alpha_{m-1} & \beta_m \\ & & & & & \beta_m & \alpha_m \end{bmatrix} \quad (3.10)$$

The matrix T_m is *uniquely* defined by the dynamic matrix $K^{-1}M$ and the starting vector q_1 (see Parlett [1980]). A set of vectors $(q_1, K^{-1} M q_1, \dots, (K^{-1} M)^{m-1} q_1)$, M -orthonormalized by Gram-Schmidt procedure in recurrence equations (3.7), forms *Lanczos vector basis* which spans Krylov subspace. Additional possibility to span the same Krylov subspace is given by *Ritz vector basis* $(\Psi_1, \Psi_2, \dots, \Psi_m)$ which can be formed after the standard eigenvalue problem for T_m is solved

$$T_m S_m = \Omega_m^{-2} S_m \quad (3.11)$$

$$\Psi = Q S_m \quad (3.12)$$

The complete summary of the algorithm is given in table 3.1, at the end of this section.

If we choose Ritz vector basis to span the subspace, the modal transformation is $u(t) = \Psi y(t)$ and the set of modal equations of motion could be restated as

$$\ddot{y}(t) + C_m \dot{y}(t) + \Omega_m^2 y(t) = f_m g(t) \quad (3.13)$$

where

$$\Psi_m^T M \Psi_m = I \quad (3.14)$$

$$\Psi_m^T C \Psi_m = C_m \quad (3.15)$$

$$\Psi_m^T K \Psi_m = \Omega_m^2 = \text{diag}(\omega_i^2) \quad (3.16)$$

$$\Psi_m^T f g(t) = f_m g(t) \quad (3.17)$$

Because of the non-proportional nature of damping matrix, equations of motion remain coupled after transformation to Ritz generalized (modal) coordinates. Efficient numerical algorithm, devised in Ibrahimbegovic and Wilson [1988], is then used for the solution of system (3.13). First the additive split of modal damping matrix $C_m = \text{diag}(2 \xi \omega) + \hat{C}_m$ is introduced and the system is rewritten in the form

$$\ddot{y}(t) + \text{diag}(2 \xi \omega_i) \dot{y}(t) + \Omega_m^2 y(t) = f_m g(t) - \sum \hat{C}_m \dot{y}(t) \quad (3.18)$$

System of equations (3.18) is then solved by iteration. The complete summary of the iterative procedure is presented in table 3.2.

Table 3.1 Load dependent vector algorithm - real Ritz vector basis

Step 1 : Pick a starting vector	Operation count
$\text{solve } \mathbf{K} \mathbf{q} = \mathbf{f}$ $\mathbf{p} = \mathbf{M} \mathbf{q}$ $\beta_1 = (\mathbf{q}^T \mathbf{p})^{1/2}$ $\mathbf{q} \leftarrow \mathbf{q}/\beta_1$ $\mathbf{p} \leftarrow \mathbf{p}/\beta_1$ $\text{solve } \mathbf{K} \mathbf{r} = \mathbf{p}$ $\alpha_1 = (\mathbf{r}^T \mathbf{p})$ $\mathbf{r} \leftarrow \mathbf{r} - \alpha_1 \mathbf{q}$ $\text{oldp} = \mathbf{M} \mathbf{r}$ $\beta_2 = (\mathbf{r}^T \text{oldp})^{1/2}$ $\text{store } \mathbf{q} \text{ as } \mathbf{q}_1$	$v(\mathbf{K})^\dagger$ $\mu(\mathbf{M})^\S$ n n n $v(\mathbf{K})$ n n $\mu(\mathbf{M})$ n
Loop : For $j = 2, 3, \dots, m$	Operation count
$\text{oldq} \leftarrow \mathbf{q}$ $\mathbf{p} \leftarrow \text{oldp}$ $\mathbf{q} \leftarrow \mathbf{r}/\beta_j$ $\mathbf{p} \leftarrow \mathbf{p}/\beta_j$ $\text{solve } \mathbf{K} \mathbf{r} = \mathbf{p}$ $\alpha_j = (\mathbf{r}^T \mathbf{p})$ $\mathbf{r} \leftarrow \mathbf{r} - \alpha_j \mathbf{q}$ $\mathbf{r} \leftarrow \mathbf{r} - \beta_j \text{oldq}$ $\text{oldp} = \mathbf{M} \mathbf{r}$ $\beta_{j+1} = (\mathbf{r}^T \text{oldp})^{1/2}$ $\text{store } \mathbf{q} \text{ as } \mathbf{q}_j$	n n $v(\mathbf{K})$ n n n $\mu(\mathbf{M})$ n
After m steps	Operation count
$\text{Solve } \mathbf{T}_m \mathbf{S}_m = \Omega_m^{-2} \mathbf{S}_m$ $\text{Form Ritz vector basis } \Psi = \mathbf{Q} \mathbf{S}_m$	$10m^3$ nm^2

$\dagger v(\mathbf{K})$ represents the number of operations to solve $\mathbf{K} \mathbf{y} = \mathbf{x}$
 $\S \mu(\mathbf{M})$ represent the number of operation to compute $\mathbf{M} \mathbf{x}$

Table 3.2- Algorithm for the integration of modal equations
for systems with non-proportional damping

A. Initial Computations :

1. Precompute exponential and trigonometric expressions for constant time step
 $\Delta t = t_1 - t_0$

$$B_{i1} = e^{-\xi_i \omega_i \Delta t} \cos \omega_{Di} \Delta t$$

$$B_{i2} = e^{-\xi_i \omega_i \Delta t} \sin \omega_{Di} \Delta t$$

B. For each time step ($\Delta t = t_1 - t_0$) :

1. Set initial condition for iteration process

$$\dot{y}^{(0)}(t_1) = y(t_0)$$

2. Compute loading

$$f_i(t) = a + b t, \quad \text{where : } a = f_i(t_0) \quad b = \frac{f_i(t_1) - f_i(t_0)}{\Delta t}$$

C. Iterate through the number of modes :

1. Compute off-diagonal damping forces

$$\left(\hat{C}_m y^{(k-1)}(t) \right)_i = c + d t$$

2. Update loading

$$a \leftarrow a - c, \quad b \leftarrow b - d$$

3. Compute coefficients

$$A_0 = \frac{a}{\omega_i^2} - \frac{2 \xi_i b}{\omega_i^3}, \quad A_1 = b / \omega_i^2$$

$$A_2 = y_i(t_0) - A_0$$

$$A_3 = \frac{1}{\omega_{Di}} \left(\dot{y}_i(t_0) + \xi_i \omega_i A_2 - A_1 \right)$$

4. Compute the new values for displacements and velocities

$$y_i^{(k)}(t_1) = A_0 + A_1 \Delta t + A_2 B_{i1} + A_3 B_{i2}$$

$$\dot{y}_i^{(k)}(t_1) = A_1 + \left(\omega_{Di} A_3 - \xi_i \omega_i A_2 \right) B_{i1} - \left(\omega_{Di} A_2 + \xi_i \omega_i A_3 \right) B_{i2}$$

5. Check convergence

$$\text{if : } \left| \dot{y}^{(k)}(t_1) - \dot{y}^{(k-1)}(t_1) \right|_{\infty} / \left| \dot{y}^{(k)}(t_1) \right|_{\infty} \leq \text{tol.}$$

4. COMPLEX VECTOR BASIS

Theoretical basis for formation of the complex vector basis that will uncouple equations of motion (2.1), for the case of non-proportional damping, was introduced three decades ago by Foss [1958]. Additional publications (e.g. Veletsos and Ventura [1986]) tried to provide some physical insight into the use of complex vector basis aiming to raise the popularity of the method in the engineering community. However, in addition to the lack of physical understanding, the equally important reason for the rare use of complex vector basis is that the method tends to be computationally very expensive for practical large systems. Quite recently devised Lanczos algorithm in Chen [1987] for the solution of quadratic eigenvalue problems can ease the burden of large computational expense.

Only a short summary of the algorithm we use to generate complex vector basis is given here. For more thorough discussion the reader is referred to Chen and Taylor [1988].

To generate the complex Ritz vector basis, the second order differential equation is transformed into a first order one (see Frazer et al. [1946]) as

$$\mathbf{A} \dot{\tilde{\mathbf{u}}}(t) + \mathbf{B} \tilde{\mathbf{u}}(t) = \tilde{\mathbf{f}} g(t) \quad (4.1)$$

where

$$\mathbf{A} = \begin{bmatrix} \mathbf{C} & \mathbf{M} \\ \mathbf{M} & \mathbf{0} \end{bmatrix} \quad \mathbf{B} = \begin{bmatrix} \mathbf{K} & \mathbf{0} \\ \mathbf{0} & -\mathbf{M} \end{bmatrix} \quad (4.2)$$

and

$$\tilde{\mathbf{u}}(t) = \begin{bmatrix} \mathbf{u}(t) \\ \dot{\mathbf{u}}(t) \end{bmatrix} \quad \tilde{\mathbf{f}} = \begin{bmatrix} \mathbf{f} \\ \mathbf{0} \end{bmatrix} \quad (4.3)$$

The equations (4.2) are not the only first order form of (2.1); however, they are the most suitable for our purpose. Note that \mathbf{A} and \mathbf{B} in equations (4.2) are symmetric (induced by the symmetry of \mathbf{M} , \mathbf{C} and \mathbf{K}). However, neither \mathbf{A} nor \mathbf{B} are positive definite. Hence

$$(\tilde{\mathbf{q}}_i, \tilde{\mathbf{q}}_i)_{\mathbf{A}} = \tilde{\mathbf{q}}_i^T \mathbf{A} \tilde{\mathbf{q}}_i \quad (4.4)$$

is not always positive for $\tilde{\mathbf{q}}_i \neq \mathbf{0}$. Although we keep formally the same load dependent vector algorithm (with appropriate quantities of size $2n$ instead of n denoted by $(\tilde{\cdot})$), we have to warn about the dangers of utilizing *improper* (or *indefinite*) inner product (4.4). Namely, a set of orthogonal vectors may be linearly dependent, a nonzero vector can have zero norm and the reduced system can become unstable even though the original system is stable (see Chen and Taylor [1988]).

A variant of the standard load dependent algorithm can be constructed (see Chen [1987]) to generate an \mathbf{A} -orthogonal set of vectors by applying the Gram-Schmidt orthogonalization procedure on the Krylov subspace spanned by

$(\tilde{\mathbf{q}}_1, \mathbf{D}\tilde{\mathbf{q}}_1, \mathbf{D}^2\tilde{\mathbf{q}}_1, \dots, \mathbf{D}^{\tilde{m}-1}\tilde{\mathbf{q}}_1)$, where the new dynamic matrix is $\mathbf{D} = \mathbf{B}^{-1} \mathbf{A}$. The starting vector $\tilde{\mathbf{q}}_1$ is \mathbf{A} -normalized static response to fixed spatial loading distribution, i.e.

$$\tilde{\mathbf{r}}_1 = \mathbf{B}^{-1} \tilde{\mathbf{f}} = \begin{bmatrix} \mathbf{K}^{-1}\mathbf{f} \\ \mathbf{0} \end{bmatrix} \quad (4.5)$$

$$\delta_1 = \tilde{\mathbf{r}}_1^T \mathbf{A} \tilde{\mathbf{r}}_1 / |\tilde{\mathbf{r}}_1^T \mathbf{A} \tilde{\mathbf{r}}_1| \quad (4.6)$$

$$\gamma_1 = |\tilde{\mathbf{r}}_1^T \mathbf{A} \tilde{\mathbf{r}}_1|^{1/2} \quad (4.7)$$

$$\tilde{\mathbf{q}}_1 = \tilde{\mathbf{r}}_1 / \gamma_1 \quad (4.8)$$

The three-term recurrence formula now is

$$\gamma_{j+1} \tilde{\mathbf{q}}_{j+1} = \tilde{\mathbf{r}}_{j+1} = \mathbf{B}^{-1} \mathbf{A} \tilde{\mathbf{q}}_j - \alpha_j \tilde{\mathbf{q}}_j - \beta_j \tilde{\mathbf{q}}_{j-1} \quad (4.9)$$

where

$$\alpha_j = \delta_j \tilde{\mathbf{q}}_j^T \mathbf{A} \mathbf{B}^{-1} \mathbf{A} \tilde{\mathbf{q}}_j \quad (4.10)$$

$$\beta_j = \delta_j \tilde{\mathbf{q}}_{j-1}^T \mathbf{A} \mathbf{B}^{-1} \mathbf{A} \tilde{\mathbf{q}}_j \quad (4.11)$$

$$\delta_{j+1} = \tilde{\mathbf{r}}_{j+1}^T \mathbf{A} \tilde{\mathbf{r}}_{j+1} / |\tilde{\mathbf{r}}_{j+1}^T \mathbf{A} \tilde{\mathbf{r}}_{j+1}| \quad (4.12)$$

$$\gamma_{j+1} = |\tilde{\mathbf{r}}_{j+1}^T \mathbf{A} \tilde{\mathbf{r}}_{j+1}|^{1/2} \quad (4.13)$$

where δ_j , being +1 or -1, appears as a consequence of \mathbf{A} being indefinite matrix.

The dimension of the Lanczos vectors $\tilde{\mathbf{q}}_j$ here is $2n$ instead of n . However, the cost of computing these Lanczos vectors is not doubled because the structure of the matrices \mathbf{A} and \mathbf{B} can be exploited.

After $\tilde{m} = 2m$ steps, we have the Lanczos vectors $\tilde{\mathbf{Q}} = [\tilde{\mathbf{q}}_1, \dots, \tilde{\mathbf{q}}_{\tilde{m}}]$ satisfying the following relation

$$\tilde{\mathbf{Q}}^T \mathbf{A} \tilde{\mathbf{Q}} = \mathbf{\Delta} \quad (4.14)$$

and

$$\tilde{\mathbf{Q}}^T \mathbf{A} \mathbf{B}^{-1} \mathbf{A} \tilde{\mathbf{Q}} = \mathbf{\Delta} \tilde{\mathbf{T}}_{\tilde{m}} \quad (4.15)$$

where $\mathbf{\Delta}$ is an $2m \times 2m$ diagonal matrix with the diagonal elements δ_j , and $\tilde{\mathbf{T}}_{\tilde{m}}$ is a tridiagonal matrix

$$\tilde{\mathbf{T}}_{\tilde{m}} = \begin{bmatrix} \alpha_1 & \beta_2 & & & & \\ \gamma_2 & \alpha_2 & \beta_3 & & & \\ & & \cdot & \cdot & & \\ & & & \gamma_{\tilde{m}-1} & \alpha_{\tilde{m}-1} & \beta_{\tilde{m}} \\ & & & & \gamma_{\tilde{m}} & \alpha_{\tilde{m}} \end{bmatrix} \quad (4.16)$$

The Ritz vectors are computed from $\tilde{\Psi} = \tilde{\mathbf{Q}} \tilde{\mathbf{S}}_{\tilde{m}}$, where $\tilde{\mathbf{S}}_{\tilde{m}}$ is the solution for eigenvectors of the following eigenproblem

$$\Delta \tilde{\mathbf{T}}_{\tilde{m}} \tilde{\mathbf{S}}_{\tilde{m}} = \Delta \tilde{\mathbf{S}}_{\tilde{m}} \tilde{\mathbf{\Omega}}_{\tilde{m}}^{-1} \quad (4.17)$$

Note that $\mathbf{T}_{\tilde{m}}$ is a real matrix, but $\tilde{\mathbf{\Omega}}_{\tilde{m}}^{-1}$ contains complex eigenvalues (Ritz values). Hence, complex arithmetics is not needed until the last moment.

Using the transformation $\tilde{\mathbf{u}}(t) = \tilde{\Psi} \tilde{\mathbf{y}}(t)$, we can obtain the uncoupled form of the equations of motion (2.1)

$$\ddot{\tilde{y}}_j(t) - \tilde{\omega}_j \tilde{y}_j(t) = \tilde{f}_{\tilde{m}_j}(t) \quad (4.18)$$

where both the $\tilde{\omega}_j$ and the $\tilde{f}_{\tilde{m}_j}(t)$ are complex-valued for underdamped modes.

For the piece-wise linear variation of excitation, exact solution of equation (4.18) can be then utilized in the computational process (see Chen and Taylor [1988]). The complete summary of the load dependent vector algorithm is given in table 4.1.

Table 4.1 Load dependent vector algorithm - complex Ritz vector basis

Step 1 : Pick a starting vector	Operation count
$solve \mathbf{B} \mathbf{q} = \tilde{\mathbf{f}}$	$v(\mathbf{K})^\dagger$
$\mathbf{p} = \mathbf{A} \mathbf{q}$	$2\mu(\mathbf{M}) + \mu(\mathbf{C})^\S$
$\gamma_1 = \mathbf{q}^T \mathbf{p} ^{1/2}$	$2n$
$\delta_1 = (\mathbf{q}^T \mathbf{p}) / \mathbf{q}^T \mathbf{p} $	
$\mathbf{p} \leftarrow \mathbf{p}/\gamma_1$	$2n$
$\mathbf{q} \leftarrow \mathbf{q}/\gamma_1$	$2n$
$solve \mathbf{B} \mathbf{r} = \mathbf{p}$	$v(\mathbf{K}) + v(\mathbf{M})$
$\alpha_1 = (\mathbf{r}^T \mathbf{p}) \delta_1$	$2n$
$\mathbf{r} \leftarrow \mathbf{r} - \alpha_1 \mathbf{q}$	$2n$
$\mathbf{oldp} = \mathbf{A} \mathbf{r}$	$2\mu(\mathbf{M}) + \mu(\mathbf{C})$
$\gamma_2 = \mathbf{r}^T \mathbf{oldp} ^{1/2}$	$2n$
$\delta_2 = (\mathbf{r}^T \mathbf{oldp}) / \mathbf{r}^T \mathbf{oldp} ^{1/2}$	
store \mathbf{q} as $\tilde{\mathbf{q}}_1$	
Loop : For $j = 2, 3, \dots, 2m$	Operation count
$\mathbf{oldq} \leftarrow \mathbf{q}$	
$\mathbf{oldp} \leftarrow \mathbf{p}$	
$\mathbf{q} \leftarrow \mathbf{r}/\gamma_j$	$2n$
$\mathbf{p} \leftarrow \mathbf{p}/\gamma_j$	$2n$
$solve \mathbf{B} \mathbf{r} = \mathbf{p}$	$v(\mathbf{K}) + v(\mathbf{M})$
$\alpha_j = (\mathbf{r}^T \mathbf{p}) \delta_j$	$2n$
$\beta_j = (\mathbf{r}^T \mathbf{oldp}) \delta_j$	$2n$
$\mathbf{r} \leftarrow \mathbf{r} - \alpha_j \mathbf{q}$	$2n$
$\mathbf{r} \leftarrow \mathbf{r} - \beta_j \mathbf{oldq}$	$2n$
$\mathbf{oldp} = \mathbf{A} \mathbf{r}$	$2\mu(\mathbf{M}) + \mu(\mathbf{C})$
$\gamma_{j+1} = \mathbf{r}^T \mathbf{oldp} ^{1/2}$	$2n$
$\delta_{j+1} = (\mathbf{r}^T \mathbf{oldp}) / \mathbf{r}^T \mathbf{oldp} ^{1/2}$	
store \mathbf{q} as $\tilde{\mathbf{q}}_j$	
After $2m$ steps	Operation count
Solve $\tilde{\mathbf{T}}_{\tilde{\mathbf{m}}} \tilde{\mathbf{S}}_{\tilde{\mathbf{m}}} = \tilde{\mathbf{\Omega}}_{\tilde{\mathbf{m}}}^{-1} \tilde{\mathbf{S}}_{\tilde{\mathbf{m}}}$	$10(2m)^3$
Form Ritz vector basis $\tilde{\mathbf{\Psi}} = \tilde{\mathbf{Q}} \tilde{\mathbf{S}}_{\tilde{\mathbf{m}}}$	$2n(2m)^2$

$\dagger v(\mathbf{K})$ and $v(\mathbf{M})$ represent the number of operations to solve $\mathbf{K} \mathbf{y} = \mathbf{x}$ and $\mathbf{M} \mathbf{y} = \mathbf{x}$
 $\S \mu(\mathbf{M})$ and $\mu(\mathbf{C})$ represent the number of operation to compute $\mathbf{M} \mathbf{x}$ and $\mathbf{C} \mathbf{x}$

5. NUMERICAL EXAMPLES

Two typical dynamic systems with non-proportional damping are analyzed : flexible mechanical system with concentrated dampers and a soil-structure interaction problem for a gravity dam model.

5.1. Mechanical System with Concentrated Damper

The first example studied is a frame structure presented in figure 5.1. Structure is modeled by a discrete model of 10 beam elements (each with length equals 1 m) with a total of 24 degrees of freedom.

Figure 5.1.- A damped dynamic system

Young's modulus for the beam material is taken as 500 N/m^2 , while mass density and section area and inertia are specified of unit value. The damping coefficient of the concentrated damper equals 10 N sec/m .

This structural model could be considered as a representative of a control system or a passively damped space structure. Due to the model flexibility its frequency spectrum spans from 7.64 rad/sec as the lowest frequency to 1097.49 as the highest.

To ensure that non-proportional damping arising from the damper attached to node 3 is less than *critical* (underdamped system), the procedure described in Inman and Andry [1980] is used. Namely, positive definiteness of the matrix $(2 \tilde{\mathbf{K}}^{1/2} - \tilde{\mathbf{C}})$ is checked (where : $\tilde{\mathbf{K}} = \mathbf{M}^{-1/2} \mathbf{K} \mathbf{M}^{-1/2}$, $\tilde{\mathbf{C}} = \mathbf{M}^{-1/2} \mathbf{C} \mathbf{M}^{-1/2}$).

Structure is analyzed previously by Chen and Taylor [1988] within the framework of complex Ritz vectors and eigenvectors that are generated from the first order system (12). Analysis in Chen and Taylor [1988] is performed for loading variation specified as step function. Equivalent computations were performed utilizing real vector subspace generated either by the exact eigenvectors or Ritz vectors directly from the set of second order differential equations by Ibrahimbegovic and Wilson [1988]. Two sets of 4 and 10 exact eigenvectors and 4 and 10 Ritz vectors generated from both the second and the first order system are used in analysis and compared with the exact solution (obtained with all 24 vectors included).

The same computation is repeated for another loading variation specified as 1952 Taft earthquake (ground acceleration record S69E with $\text{PGA}=0.17935 \text{ g}$ @ 3.5 sec). This loading variation is used as a representative of narrow-band excitation which is illustrated by its Fourier amplitude spectrum presented in figure 5.2.

Figure 5.2.- Fourier amplitude spectrum for 1952 Taft earthquake record S69E

Plots for horizontal displacement at node 8 computed by different number of real vectors and complex vector pairs are given in figure 5.3 for the step function loading variation and in figure 5.4 for Taft earthquake.

Figure 5.3.- Horizontal displacement at node 8 for step function loading

Figure 5.4.- Horizontal displacement at node 8 for Taft earthquake loading

From the plots presented in figure 5.4 we observe that the results computed within the subspace spanned by either 10 pairs of complex vectors or 10 real vectors are very similar (equivalent convergence properties), although, in theory, different vectors are generated. That applies both for the eigenvectors and Ritz vectors and both kinds of loading we used. Reason for that is partly due to low values of equivalent damping ratios (on average 2% for all the modes) that is computed from non-proportional damping matrix neglecting off-diagonal terms (see Warburton and Sony [1977]). However, even for the larger values of non-proportional damping, it is reasonable to assume that convergence rates for both vector bases, complex and real, will be in a very good agreement. This we demonstrate in the second example.

For the computation performed utilizing a set of 4 real Ritz vectors or 4 pairs of complex Ritz vectors much better approximation to peak response is obtained than for the adequate computation performed by eigenvectors. To illustrate that, we present the ratios of peak response computed by the different number of real vectors and complex vector pairs versus the exact solution. These results are given for both kinds of loading, step function and Taft earthquake, in table 5.1.

Table 5.1 Ratios of maximum response for different vector bases versus exact solution		
Complex vector basis		
no. vect.	step function	Taft earthquake
4 eig. v.	0.754	0.830
4 Ritz v.	1.019	1.057
10 eig. v.	1.044	1.016
10 Ritz v.	0.992	0.994
Real vector basis		
no. vect.	step function	Taft earthquake
4 eig. v.	0.775	0.850
4 Ritz v.	0.928	1.057
10 eig. v.	1.046	1.017
10 Ritz v.	1.011	0.999

5.2. Pine Flat Dam - Soil-Structure Interaction

A typical soil-structure interaction problem that arises in dynamic response analysis of dam structure is presented in this example. Analysis is carried out utilizing added motion approach first described in Clough and Penzien [1975]. Detailed derivation of equation of motion is presented in Clough and Penzien [1975] and

only its final form is presented below

$$\mathbf{M} \ddot{\mathbf{u}}(t) + \mathbf{C} \dot{\mathbf{u}}(t) + \mathbf{K} \mathbf{u}(t) = \mathbf{M}_a \mathbf{R} \ddot{u}_g(t) \quad (5.1)$$

where \mathbf{M} , \mathbf{C} and \mathbf{K} are again mass, damping and stiffness matrices of complete interacting system, $\mathbf{u}(t)$ are dynamic nodal displacements, while loading takes the form of added structure "directional" mass $\mathbf{M}_a \mathbf{R}$ (in this example the dam structure) multiplied by the time variation of earthquake excitation $\ddot{u}_g(t)$. The particular form of the equation of motion (5.1) corresponds to the surface supported structures. For the embedded structures an additional loading term in the equation (5.1) appears, which corresponds to pseudo-static motion component (see Bayo and Wilson [1984]).

Rayleigh damping is used to account for energy dissipation due to material damping in dam and foundation material, constructed with the second (frequency equals 13.27 rad/sec) and the fifth mode (frequency equals 21.39 rad/sec) chosen as the control modes with modal damping ratio value equals 5%. Non-proportional nature of damping matrix arises from the concentrated viscous dampers that simulate waves radiation condition (see Laysmer and Kuhlemeyer [1969]). Distributed viscous damping is given the constant value as suggested in Cohen and Jennings [1983] as a first order approximation to the local transmitting boundary conditions (see Enquist and Majda [1977]). Nodal lumping of distributed damping values is done by row summation procedure as described in Chew [1985]. Modal transformation utilized in computation can be considered just a change of the basis (see Bathe and Wilson [1976]) and the use of transmitting boundaries is still valid. However, modal basis truncation can now be utilized to enhance computational efficiency.

Presence of overdamped modes which are the property of wave propagation problems, as described by Wolf [1985], can be checked by the procedure described in Inman and Andry [1980], applied directly to the truncated set of equations in modal coordinates. In all the runs we performed, both the complex and the real vector basis yielded the same number of overdamped modes, i.e. they both followed the same pattern. Hence, this procedure to establish the number of overdamped modes, can be used for the modal analysis that utilizes complex vector basis to *a priori* indicates the problems that may occur in that case (see Chen and Taylor [1988]).

The finite element model of dam-foundation system is presented in figure 5.5.

Figure 5.5.- Pine Flat Dam

Model of the dam used in this analysis is similar to the Pine Flat Dam analyzed for hydrodynamic effects on dams by Chakrabarti and Chopra [1973]. In this analysis hydrodynamic effects are completely disregarded. The dam and the foundation are both made of elastic homogeneous isotropic material with mechanical properties : Young's modulus 22150 MN/m^2 , mass density $2.5 \text{ kN sec}^2/\text{m}^4$ and Poisson ratio 0.25.

The computations are performed for two loading variations as in example 5.1, step function and Taft earthquake. Two sets of 5 and 10 real vectors and complex vector pairs in vector basis generated by both eigenvectors and Ritz vectors are used in computations.

As a measure for computational efficiency CPU times spent in different phases of analysis, performed on VAX II/GPX workstation under Ultrix 1.2 operating system, are presented in table 5.2

Complex vector basis			
no. vect.	Lanczos vec.	Ritz vec.	modal equations
5 eig. v.	1935.98	285.80	0.43
5 Ritz v.	570.23	27.70	0.43
10 eig. v.	2797.90	594.95	0.90
10 Ritz v.	1037.83	86.55	0.90
Real vector basis			
no. vect.	Lanczos vec.	Ritz vec.	modal equations
5 eig. v.	255.33	26.50	1.93
5 Ritz v.	71.97	4.31	1.89
10 eig. v.	391.12	52.80	4.82
10 Ritz v.	138.80	9.55	4.73

Extraction of a number of complex Ritz vector pairs requires on the average 7.75 times more effort than for the adequate number of real vectors. On the other hand, for the solution of modal equations the average CPU time ratio is inverse to the value above, which reflects the advantage of uncoupled equations set in the case of complex vector basis. However, the effort involved in the modal equations solution is overall insignificant.

For both programs, FEAP (see Taylor [1977]) and SAP (see Wilson [1980]), that we used to generate complex and real vector basis respectively, the common computational expense of factorizing stiffness matrix required 220 CPU sec (without the use of optimal equation numbering routine). Hence, from table 5.2 it is obvious that generating Ritz vector basis of 10 real vectors which yields excellent approximation to dynamic response, is merely half the effort adequate to static response computation.

To develop further appreciation for the efficiency resulting from the selection of load dependent real Ritz vector basis in modal transformation, a complete comparison of CPU time for the different phases of dynamic mode superposition analysis versus static analysis is performed. The comparison is performed for two sets of 5 and 10 real Ritz vectors, and presented in table 5.3 below. Discretization of dam model in figure 5.3 resulted in 1154 equations with the average band-width

equals 104.

solution phases	static solution	5 Ritz vec.	10 Ritz vec.
input	10.97	10.96	10.93
element stiffness	45.88	45.67	45.52
structural stiffness	11.87	11.88	11.92
factorize stiffness	220.30	220.25	220.03
Lanczos vectors	-	71.97	138.80
Ritz vectors	-	4.31	9.55
modal equations (100 steps)	-	1.89	4.73
displacement history (10 nodes)	-	2.02	3.96
stress history (10 elements)	-	446.76	461.60
nodal displacement	5.87	-	-
nodal stress (10 elements)	4.78	-	-
total time	299.67	815.71	907.04

From the table 5.3 above, we can note that the total solution process for the case of dynamic analysis triples the effort of static solution process. This seemingly unfavorable ratio results from the solution strategy of nodal stress recovery by time history of stress, which essentially requires repetition of the same computation as in the static loading case for each time step. However, for the design purposes, only the maximum values of stress and displacement are of interest. To obtain design values for earthquake input one can use a response spectrum approach for the case of non-proportional damping, such as in the problem on hands. That procedure is already introduced by Igusa and DerKiureghian [1983] as an extension of CQC method suggested first by Wilson et al. [1981] for structural systems with proportional damping. Since the time for recovery of maximum values for stress and displacement by CQC method is only slightly larger than the adequate computation for the static loading case, the ratio of the time for dynamic versus static analysis reduces to 1.5.

Displacement at the dam tip computed for a set of 5 real vectors and 5 complex vector pairs are plotted in figure 5.6 and for 10 vectors and vector pairs in figure 5.7, together with the "exact" response, obtained by the set of 100 real vectors.

Figure 5.6.- Horizontal displacement at dam tip for step function loading

Figure 5.7.- Horizontal displacement at dam tip for Taft earthquake loading

For both vector basis, real and complex, remarkable approximation properties are encountered if the Ritz vectors are used. This is illustrated in figures 5.6 and 5.7 and table 5.4.

Table 5.4 Ratios of maximum response for different vector bases versus exact solution		
Complex vector basis		
no. vect.	step function	Taft earthquake
5 eig. v.	1.121	1.029
5 Ritz v.	1.061	1.033
10 eig. v.	1.054	1.025
10 Ritz v.	1.007	1.017
Real vector basis		
no. vect.	step function	Taft earthquake
5 eig. v.	1.030	0.951
5 Ritz v.	0.965	0.987
10 eig. v.	0.969	0.978
10 Ritz v.	0.996	1.007

For the nodal displacement computation, the eigenvector basis possess almost equivalent fast convergence properties as the Ritz vector basis. However, for the accuracy in the stress recovery, Ritz vector basis is superior, as elaborated further.

Error norm for the loading spatial representation can be computed as given in Leger and Wilson [1987] by

$$\|e_f\|_2 = \frac{\|(I - M \Psi \Psi^T) f\|_2}{\|f\|_2} \times 100 \quad (\%) \quad (5.2)$$

Error norm defined by equation (5.2) is presented in table 5.5 for different numbers of real eigenvectors and real Ritz vectors used in modal transformation.

Table 5.5 Error norm for spatial loading representation	
no. vect.	error norm (%)
10 eig. v.	52.677
10 Ritz v.	24.396
100 Ritz v.	15.873

Spatial representation of loading with truncated vector basis is much better for the case of Ritz vector basis. Consequently, stresses and forces recovery is much more accurate within vector basis spanned by Ritz vectors constructed by the load dependent algorithm. To illustrate that, dam structure base shear force computed by the appropriate numbers of Ritz vectors and eigenvectors is presented in figure 5.8.

Figure 5.8.- Dam base shear force for eigenvector and Ritz vector basis - Taft earthquake

6. CLOSURE

The summary of the findings obtained in the study is :

Krylov subspace keeps its advantageous approximation properties versus exact eigenvector subspace in the case of non-proportionally damped system. This is enhanced in the case of broad band excitation.

The selection of proper load dependent real Ritz vector basis for the modal transformation, combined with an efficient method for the maximum stress recovery, reduces the total effort required for the dynamic analysis to only 1.5 times of an adequate static analysis of the same problem.

For the cases studied, the real vector basis yields comparable accuracy and convergence properties as the adequate complex vector basis, but requires much smaller CPU time for the total solution. However, the use of complex vector basis may be advantageous for the analysis to loading with time variation given as large piece-wise linear steps, where high accuracy can be ensured utilizing the exact solution of modal equations.

7. REFERENCES

- Bathe K.J. and E.L. Wilson [1976], Numerical Methods in Finite Element Analysis, Prentice-Hall, Englewood Cliffs, New Jersey
- Bayo E.P. and E.L. Wilson [1984], Finite Element and Ritz Vector Technique for the Solution of Three-Dimensional Soil-Structure Interaction Problem in the Time Domain, Eng. Comput., 1, 311-324
- Caughey T.K. [1960], Classical Normal Modes in Damped Linear Dynamic Systems, J. Appl. Mech., 27, 269-271
- Chakrabarti P. and A.K. Chopra [1973], Earthquake Analysis of Gravity Dams Including Hydrodynamic Interaction, Earthq. Engng. Struct. Dynam., 2, 143-160
- Chen H.C. [1987], Solution Methods for Damped Linear Systems, Report no. UCB/SEMM 87/08, UC Berkeley
- Chen H.C. and R.L. Taylor [1988], Solution of Viscously Damped Linear Systems Using a Set of Load-Dependent Vectors, Report no. UCB/SEMM 88/16, UC Berkeley
- Chew Y.K. [1985], Accuracy of Consistent and Lumped Viscous Dampers in Wave Propagation Problems, Int. J. Numer. Methods Eng., 52, 721-732
- Clough R.W. and J. Penzien [1975], Dynamics of Structures, McGraw-Hill, London
- Clough R.W. and S. Mojtahedi [1976], Earthquake Response Analysis Considering Non-Proportional Damping, Earthq. Engng. Struct. Dynam. 4, 489-496
- Cohen M. and P.C. Jennings [1983], Silent Boundary Methods for Transient Analysis, in 'Computational Methods for Transient Analysis' ed. T. Belytschko, T. J. R. Hughes, 302-360
- Frazer R.A., W.J. Duncan and A.R. Collar [1960], Elementary Matrices and Some Applications to Dynamics and Differential Equations, University Press, Cambridge
- Enquist B. and A. Majda [1977], Absorbing Boundary Conditions for the Numerical Simulation of Waves, Math. Comput., 31, 629-651
- Foss K.A. [1958], Co-ordinates which Uncouple the Equations of Motion of Damped Linear Dynamic System, J Appl. Mech., 25, 361-364
- Ibrahimbegovic A. and E.L. Wilson [1988], Simple Numerical Algorithms for the Mode Superposition Analysis of Discrete Linear Systems with Non-Proportional Damping, Comput. Struct., to appear
- Ibrahimbegovic A. and E.L. Wilson [1989], Spectral Content Truncation Criteria in Modal Transformation, to be published
- Igusa T and A. DerKiureghian [1983], Response Spectrum Method for System with Non-Classical Damping, Proceedings ASCE Eng. Mech. Div. Specialty Conf., Recent Advances in Engineering Mechanics and Their Application on Civil Engineering, 380-384
- Inman D.J. and A.N.jr Andry [1980], Some Results on the Nature of Eigenvalues of Discrete Damped Linear Systems, J. Appl. Mech., 47, 927-930
- Leger P. and E.L. Wilson [1987], Generation of Load Dependent Ritz Transformation Vectors in Structural Dynamic, Eng. Comput., 4, 309-318
- Lanczos C. [1950], An Iterative Method for the Solution of the Eigenvalues Problem of Linear Differential and Integral Operator, J. Res. Nat. Bur. Standards, 45, 255-282
- Laysmer J. and R.L. Kuhlemeyer [1969], Finite Dynamic Models for Infinite Media, ASCE J. Eng. Mech. Div., 95, 859-877
- Maddox N.R. [1975], On the Number of Modes Necessary for Accurate Response and Resulting Forces in Dynamic Analysis, J. Appl. Mech., 6, 516-517
- Nour-Omid B. and R.W. Clough [1984], Dynamic Analysis of Structures Using Lanczos Coordinates, Earthq. Engng. Struct. Dynam., 12, 565-577

- Parlett B.N. [1980], *The Symmetric Eigenvalue Problem*, Prentice-Hall, Englewood Cliffs, New Jersey
- Ritz W. [1909], *Über eine neue Methode zur Lösung gewisser Variationsprobleme der Mathematischen Physik*, Z. reine u. angew. Math., 135, 1-61
- Taylor R.L. [1977], *Computer Procedures for Finite Element Analysis*, in O. C. Zienkiewicz, *The Finite Element Method*, 3rd ed., chapter 24, 677-757
- Veletsos A.S. and C.E. Ventura [1986], *Modal Analysis of Non-Classically Damped Linear Systems*, Earthq. Engng. Struct. Dynam., 14, 217-243
- Warburton G.B. and S.R. Soni [1977], *Errors in Response Calculations for Non-Classically Damped Systems*, Earthq. Engng. Struct. Dynam., 5, 365-376
- Wilson E.L. and J. Penzien [1972], *Evaluation of Orthogonal Damping Matrices*, Int. J. Numer. Methods Eng., 4, 5-10
- Wilson E.L. [1977], *Numerical Methods for Dynamic Analysis*, Proceedings Int. Symposium Numer. Methods Offshore Eng., Swansea
- Wilson E.L. [1980], *SAP80 - Structural Analysis Program for Small or Large Computer Systems*, Proceedings CEPA Fall Conference
- Wilson E.L., A. DerKiureghian and E.P. Bayo [1981], *A Replacement for the SRSS Method in Seismic Analysis*, Earthq. Engng. Struct. Dynam., 9, 187-194
- Wilson E.L., M.W. Yuan and J.M. Dickens [1982], *Dynamic Analysis by Direct Superposition of Ritz Vectors*, Earthq. Engng. Struct. Dynam. 10, 813-824
- Wolf J.P. [1985], *Dynamic Soil-Structure Interaction*, Prentice-Hall, Englewood Cliffs, New Jersey

LIST OF FIGURES

Figure 5.1- A damped dynamic system

Figure 5.2- Fourier amplitude spectrum for 1952 Taft earthquake record S69E

Figure 5.3.a- Horizontal displacement at node 8 for step function loading

Figure 5.3.b- Horizontal displacement at node 8 for step function loading

Figure 5.4.a- Horizontal displacement at node 8 for Taft earthquake loading

Figure 5.4.b- Horizontal displacement at node 8 for Taft earthquake loading

Figure 5.5- Pine Flat Dam

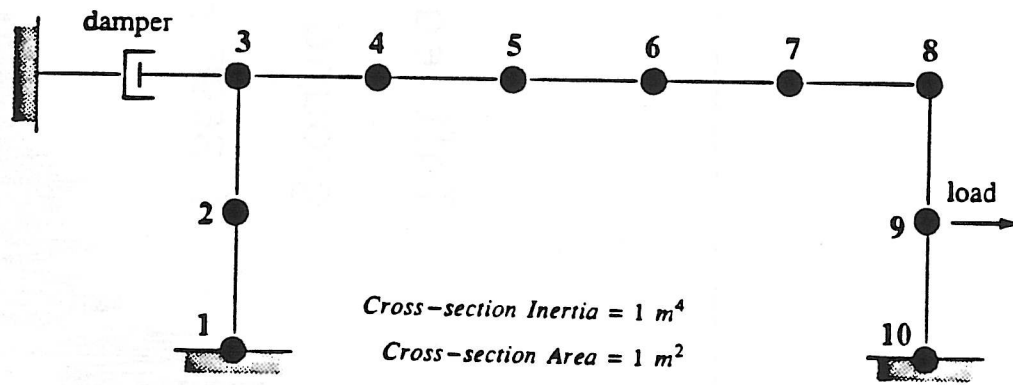
Figure 5.6.a- Horizontal displacement at dam tip for step function loading

Figure 5.6.b- Horizontal displacement at dam tip for step function loading

Figure 5.7.a- Horizontal displacement at dam tip for Taft earthquake loading

Figure 5.7.b- Horizontal displacement at dam tip for Taft earthquake loading

Figure 5.8- Dam base shear force for eigenvector and Ritz vector basis - Taft earthquake



Cross-section Inertia = 1 m⁴
Cross-section Area = 1 m²
Young's Modulus = 500 N/m²
Mass Density = 1 kg/m³
Damping Coefficient = 10 Nsec/m
f(t) = 1000 N (Heaviside function)

Figure 5.1 - A damped dynamic system

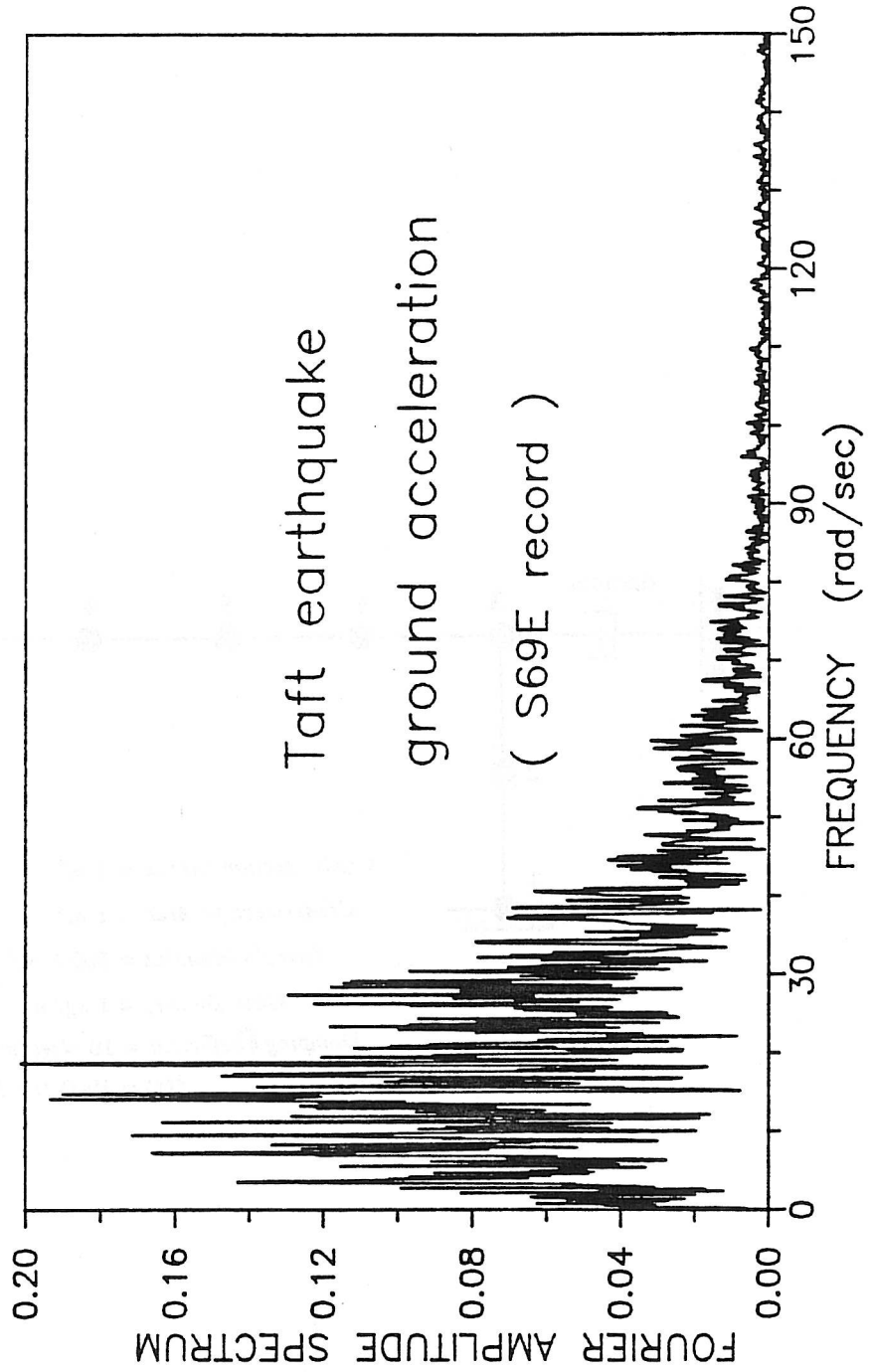
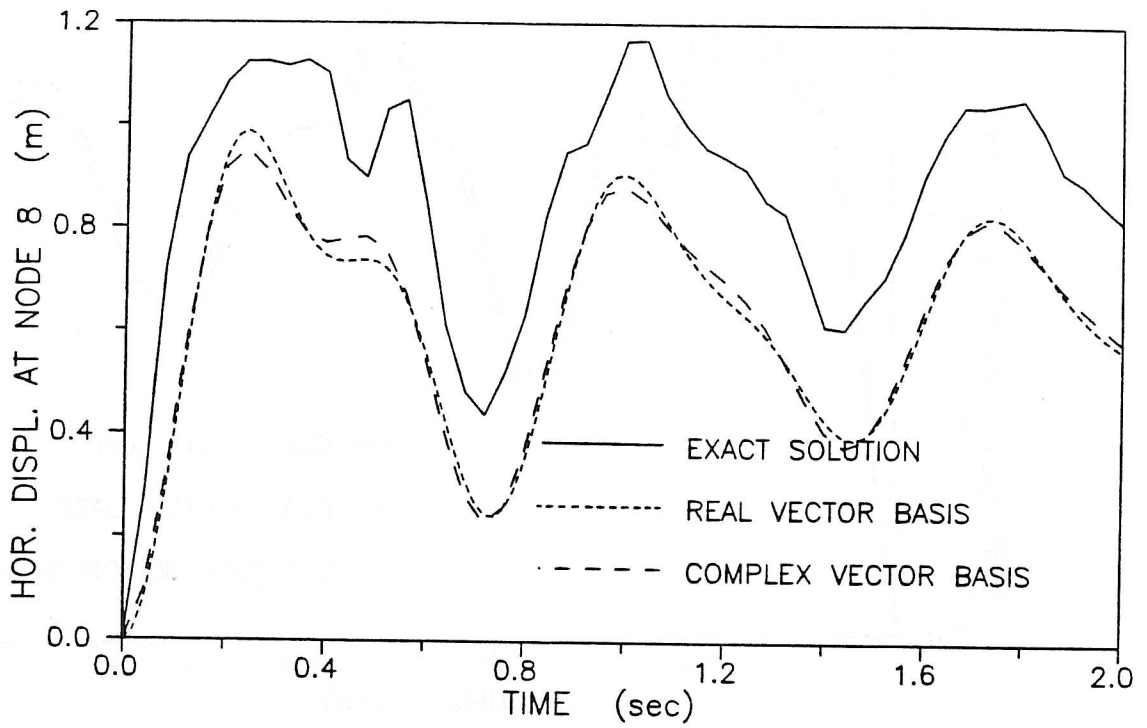


Figure 5.2 - Fourier amplitude spectrum for 1952 Taft earthquake

4 real eigenvectors and 4 complex eigenvector pairs



4 real Ritz vectors and 4 complex Ritz vector pairs

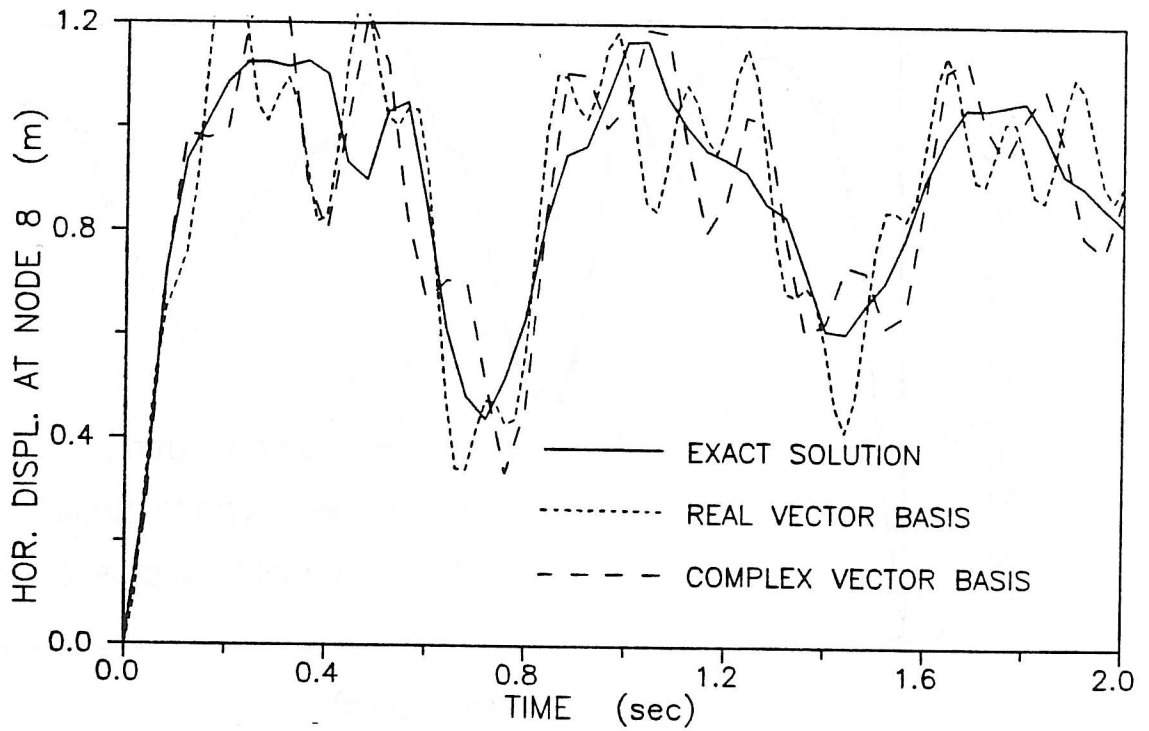
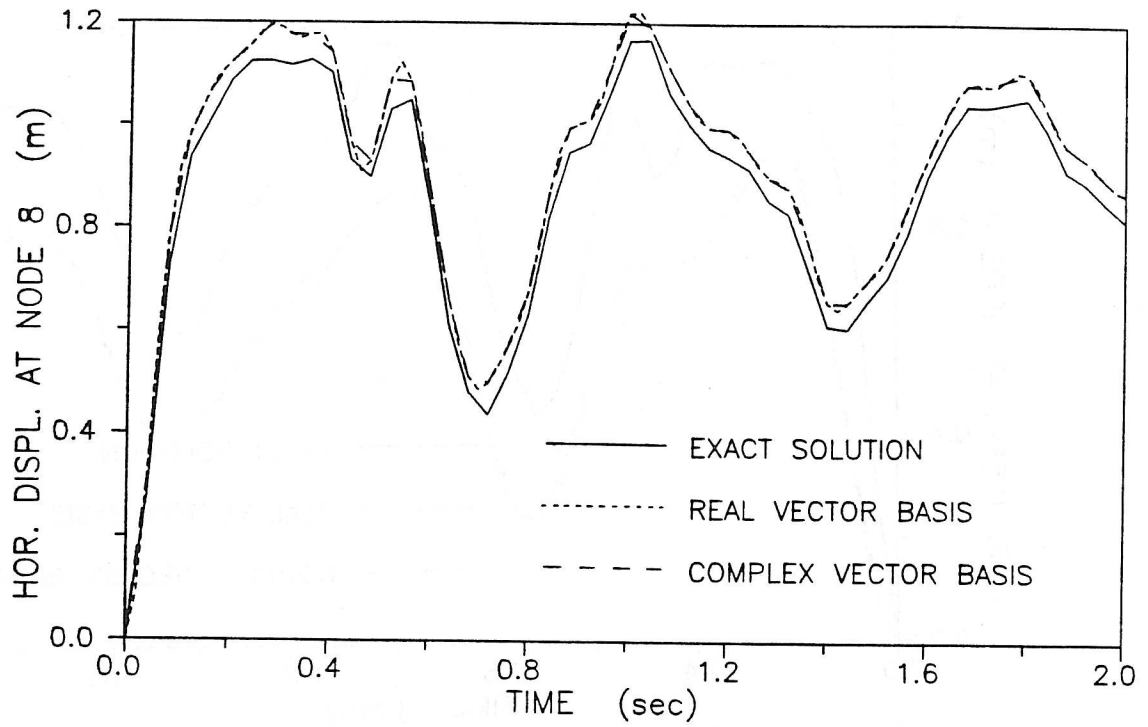


Figure 5.3.a - Horizontal displacement at node 8 for step function

10 real eigenvectors and 10 complex eigenvector pairs



10 real Ritz vectors and 10 complex Ritz vector pairs

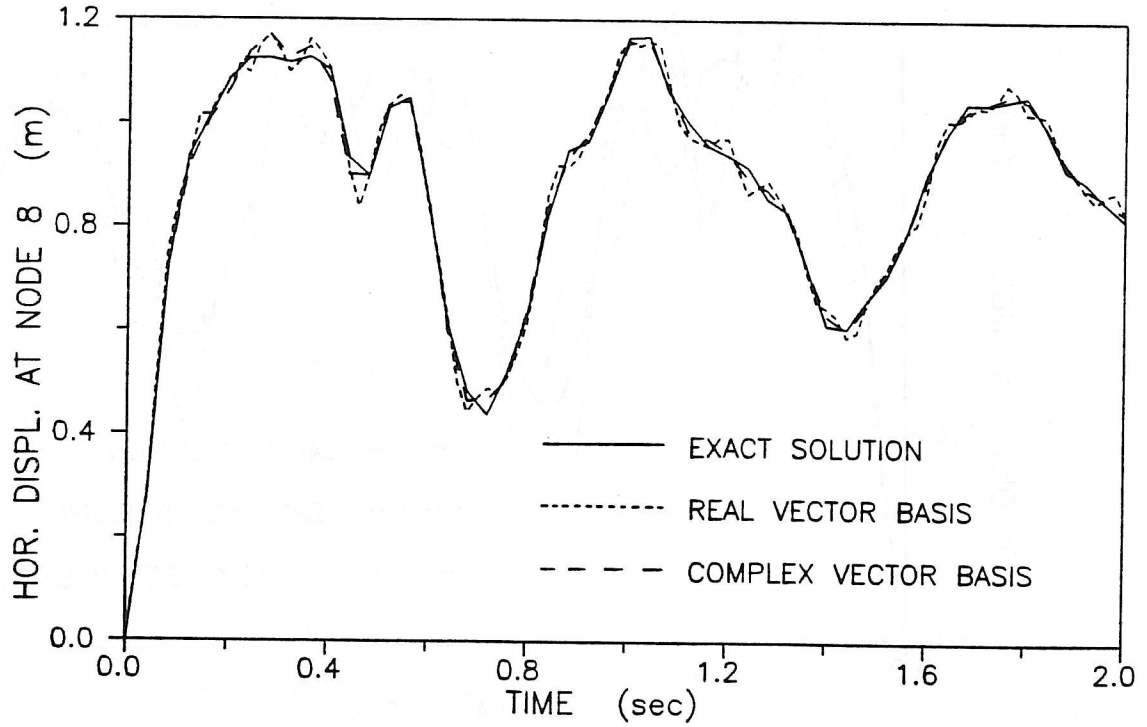
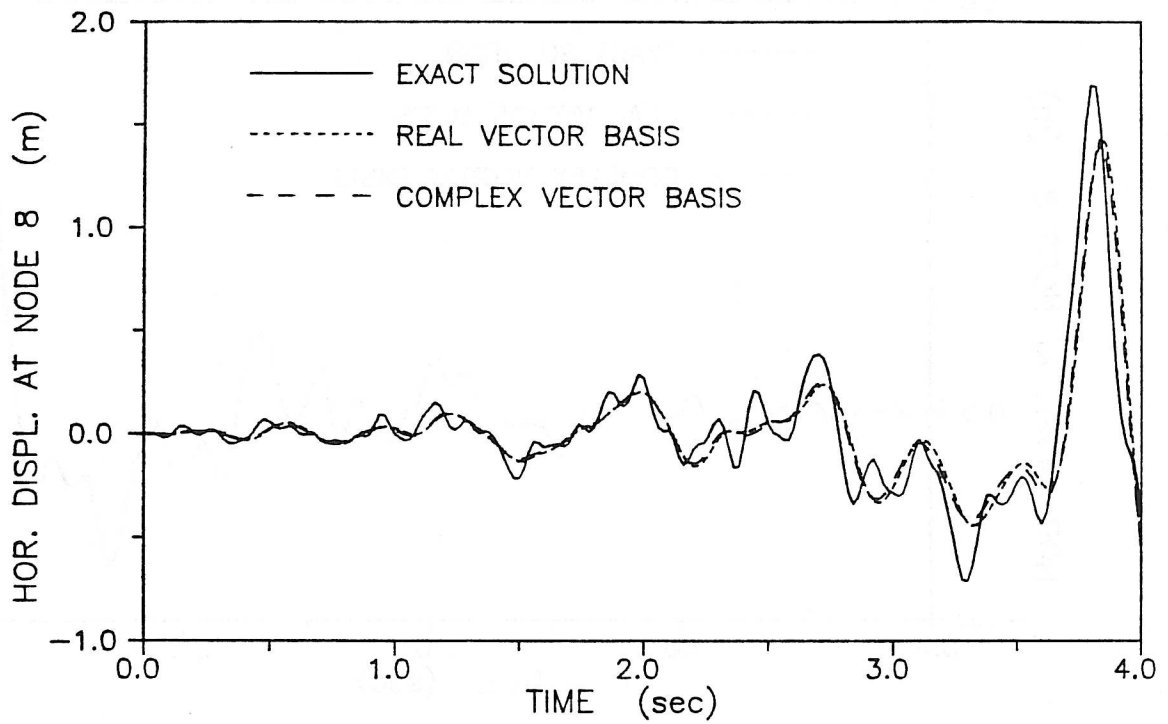


Figure 5.3.b - Horizontal displacement at node 8 for step function

4 real eigenvectors and 4 complex eigenvector pairs



4 real Ritz vectors and 4 complex Ritz vector pairs

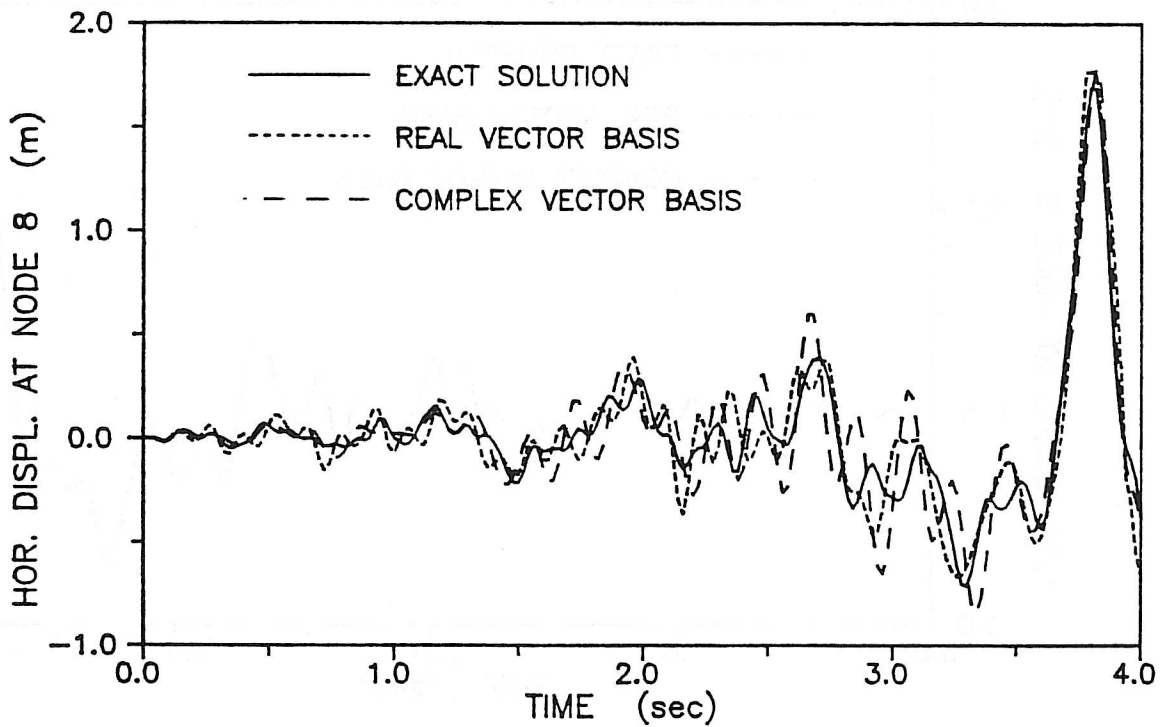
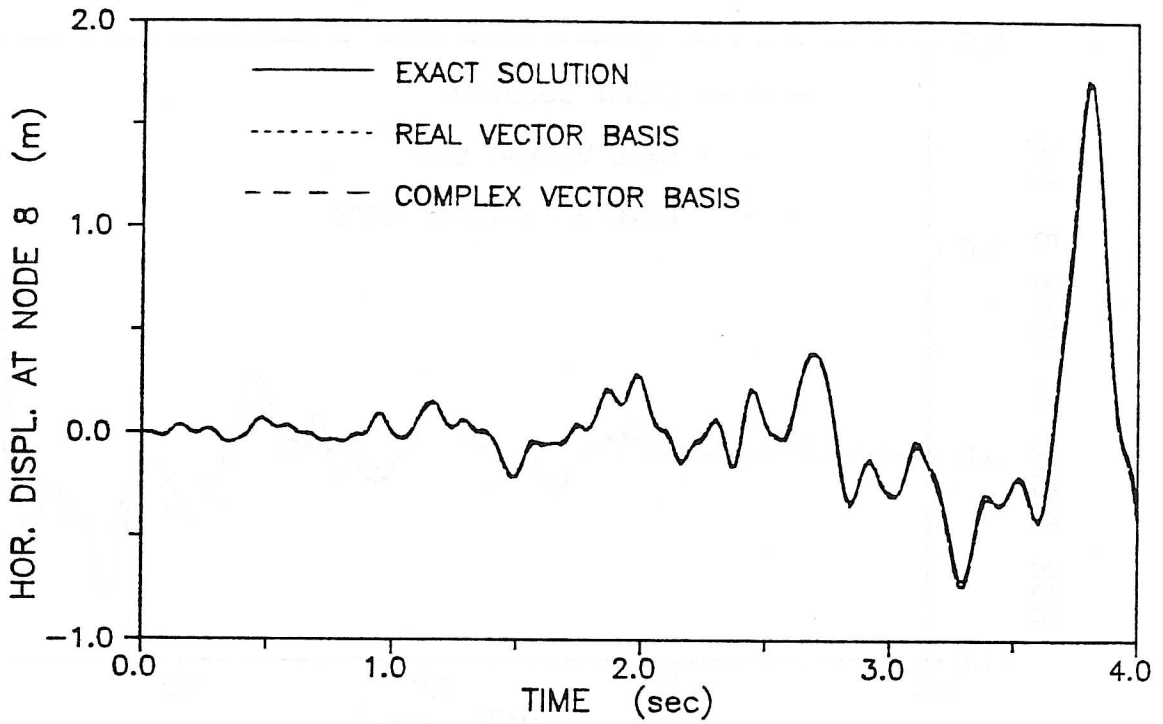


Figure 5.4.a - Horizontal displacement at node 8 for Taft earthquake

10 real eigenvectors and 10 complex eigenvector pairs



10 real Ritz vectors and 10 complex Ritz vector pairs

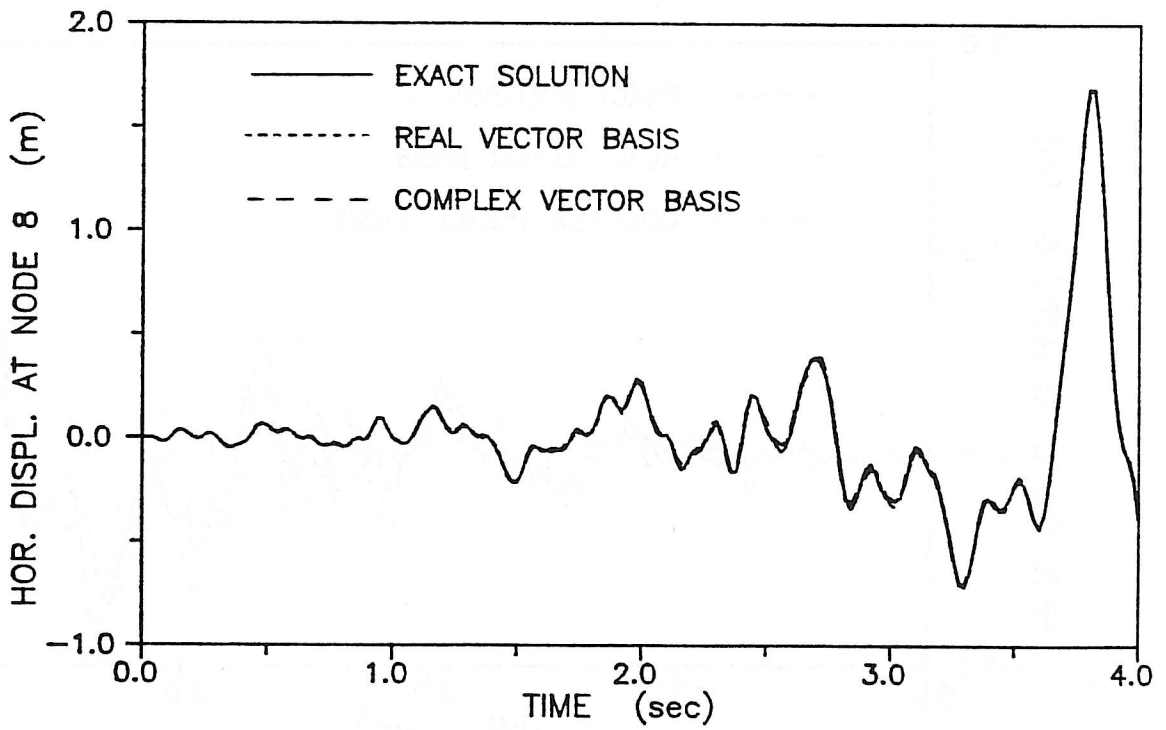


Figure 5.4.b - Horizontal displacement at node 8 for Taft earthquake

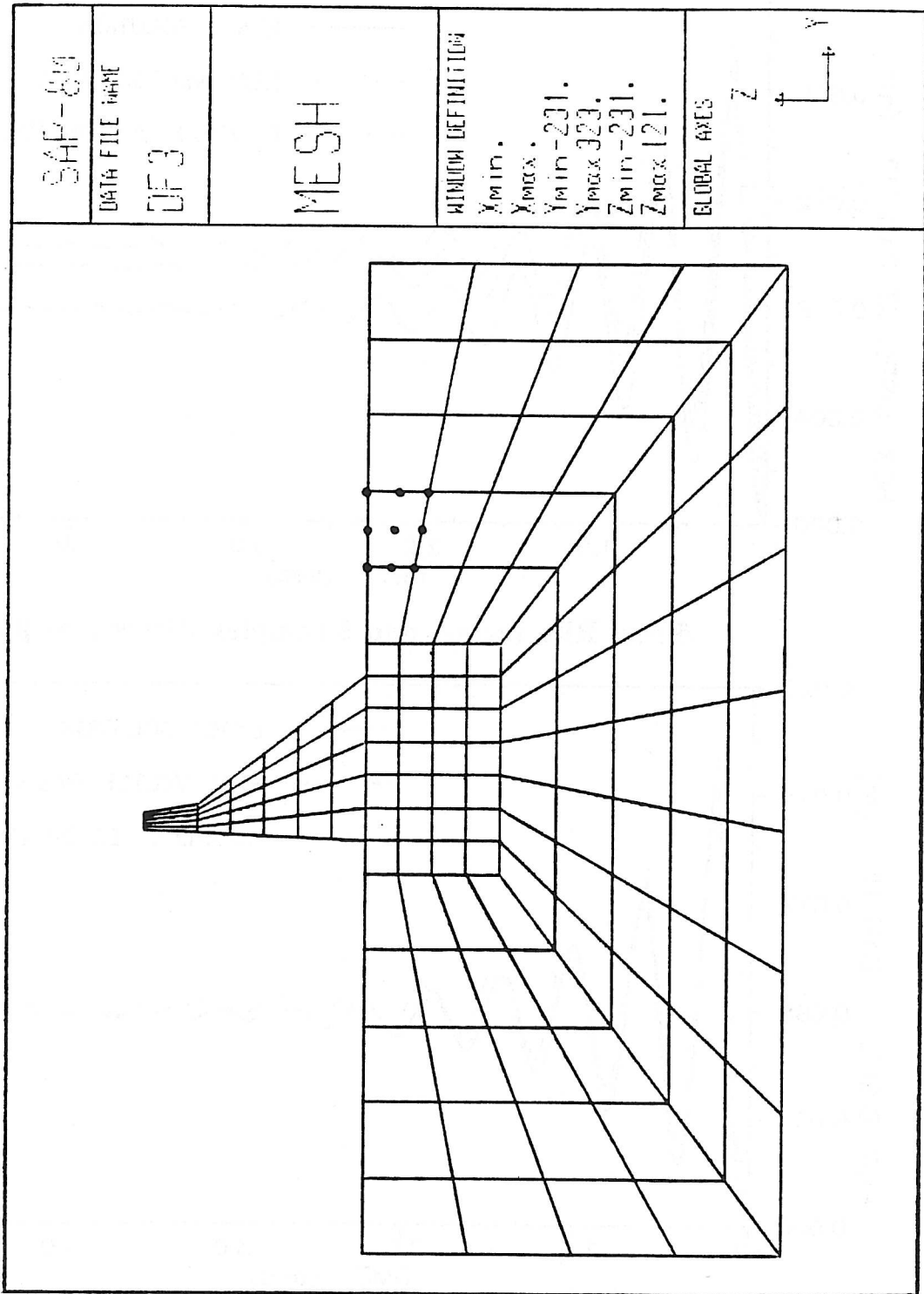
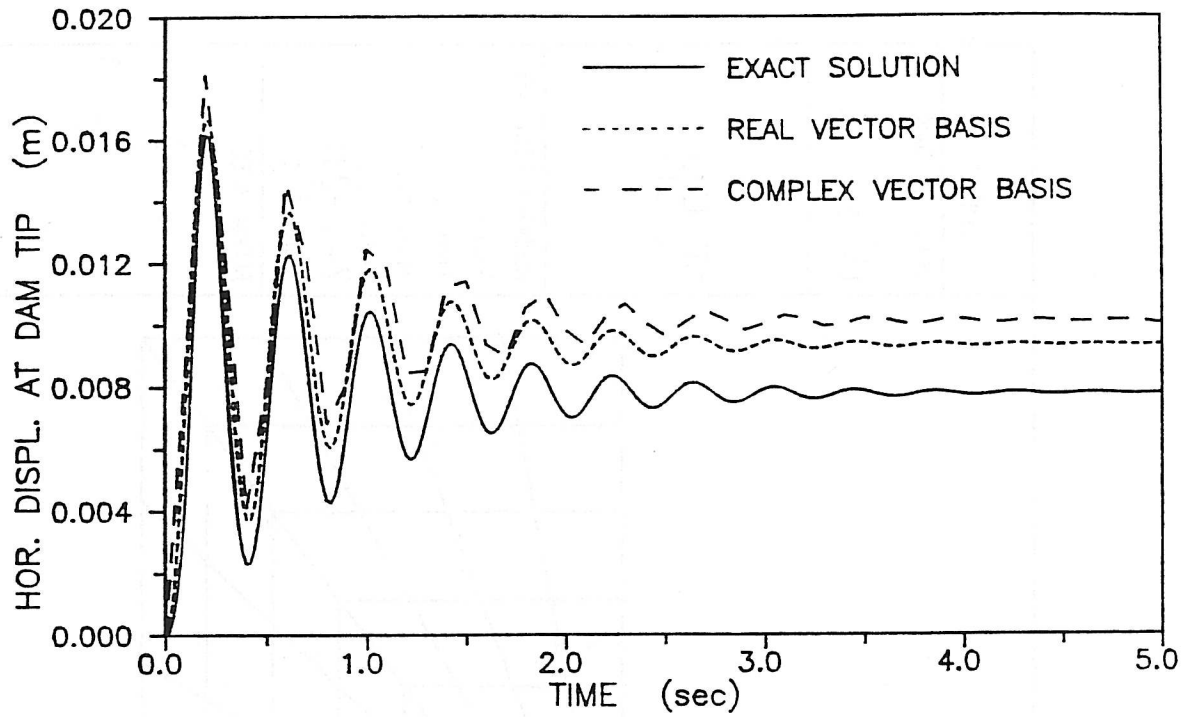


Figure 5.5 - Pine Flat Dam

5 real eigenvectors and 5 complex eigenvector pairs



5 real Ritz vectors and 5 complex Ritz vector pairs

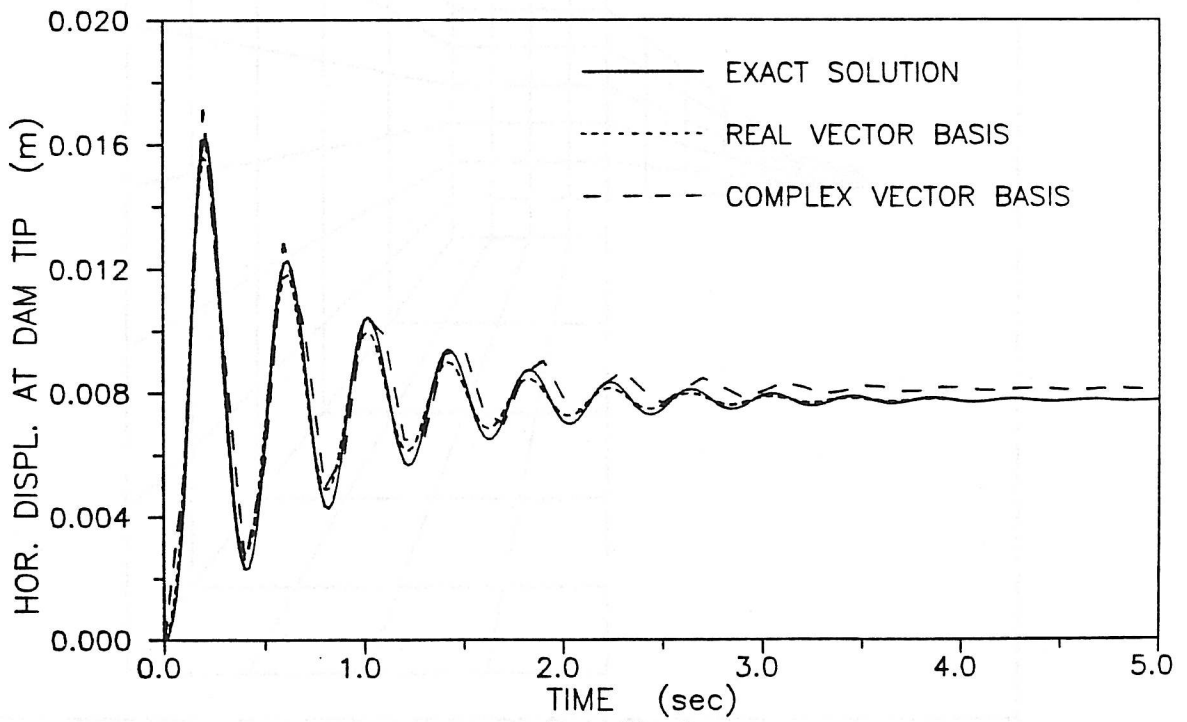
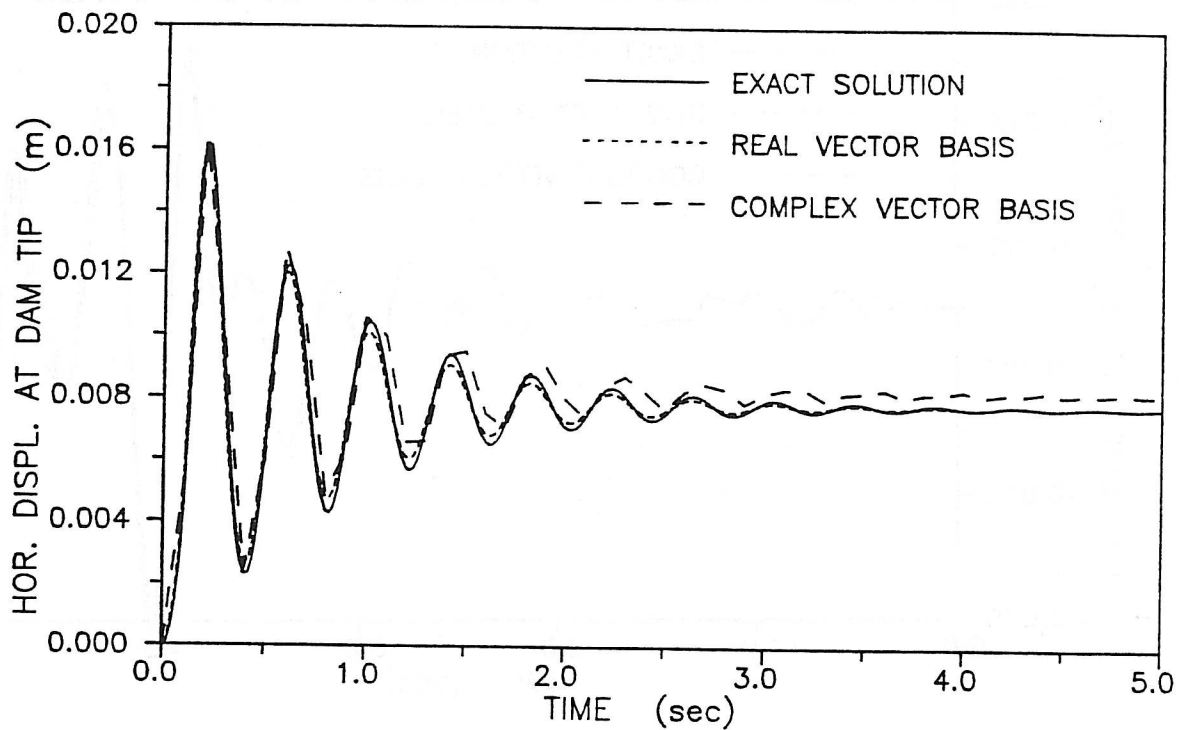


Figure 5.6.a - Horizontal displacement at dam tip for step function

10 real eigenvectors and 10 complex eigenvector pairs



10 real Ritz vectors and 10 complex Ritz vector pairs

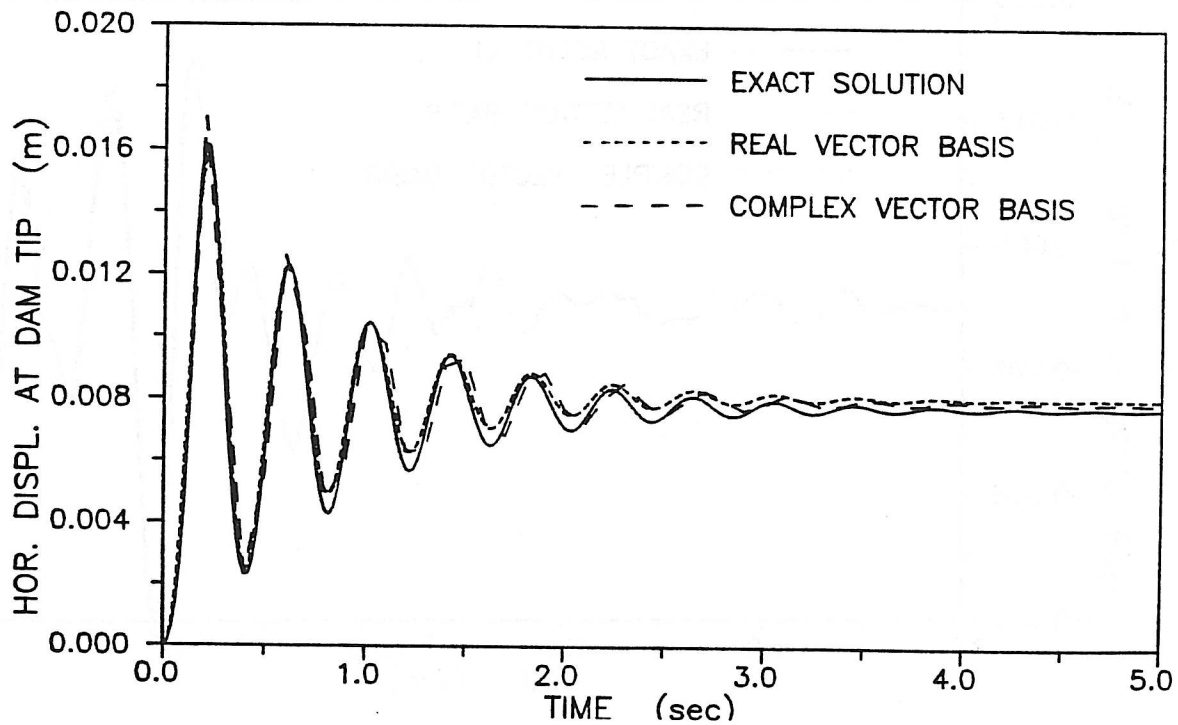


Figure 5.6.b - Horizontal displacement at dam tip for step function

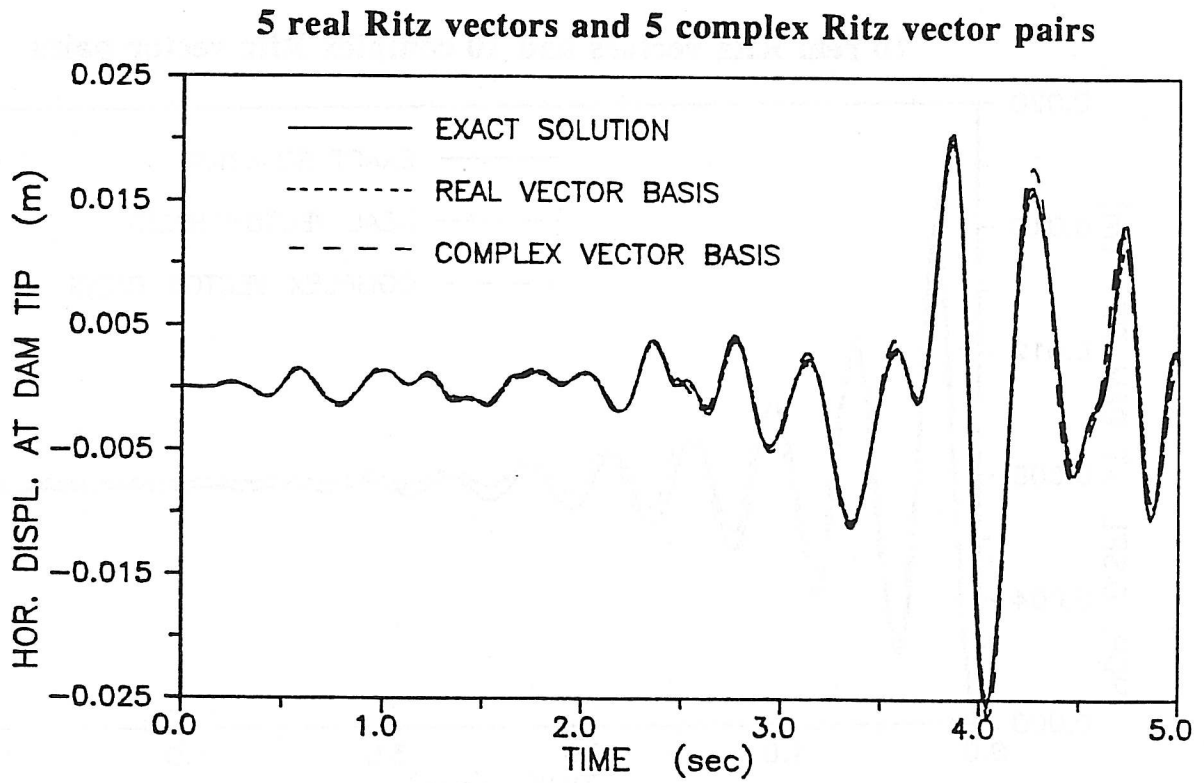
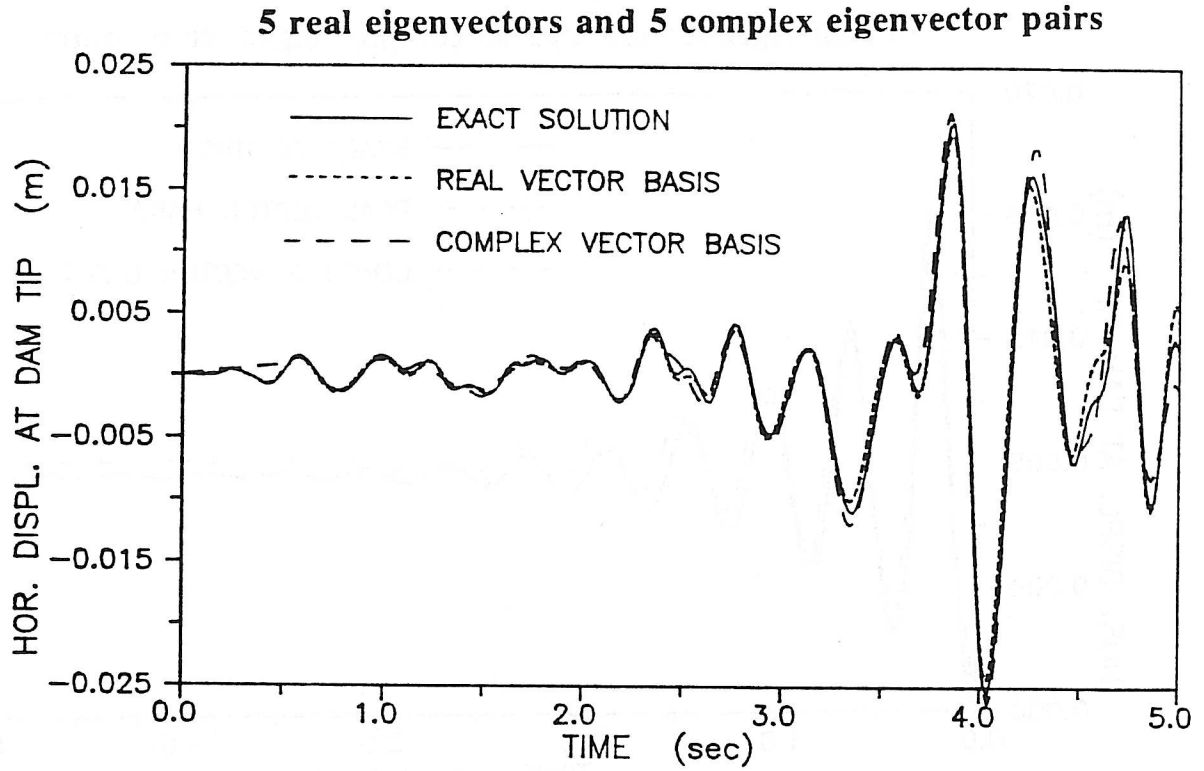
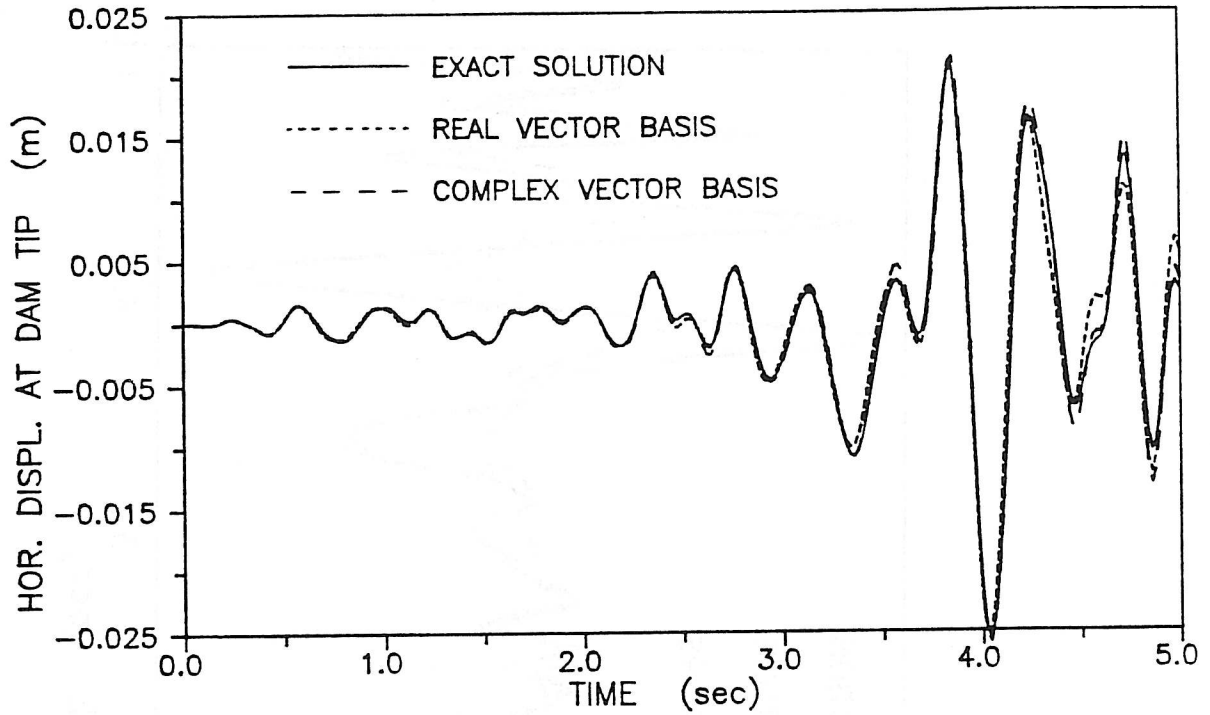


Figure 5.7.a - Horizontal displacement at dam tip for Taft earthquake

10 real eigenvectors and 10 complex eigenvector pairs



10 real Ritz vectors and 10 complex Ritz vector pairs

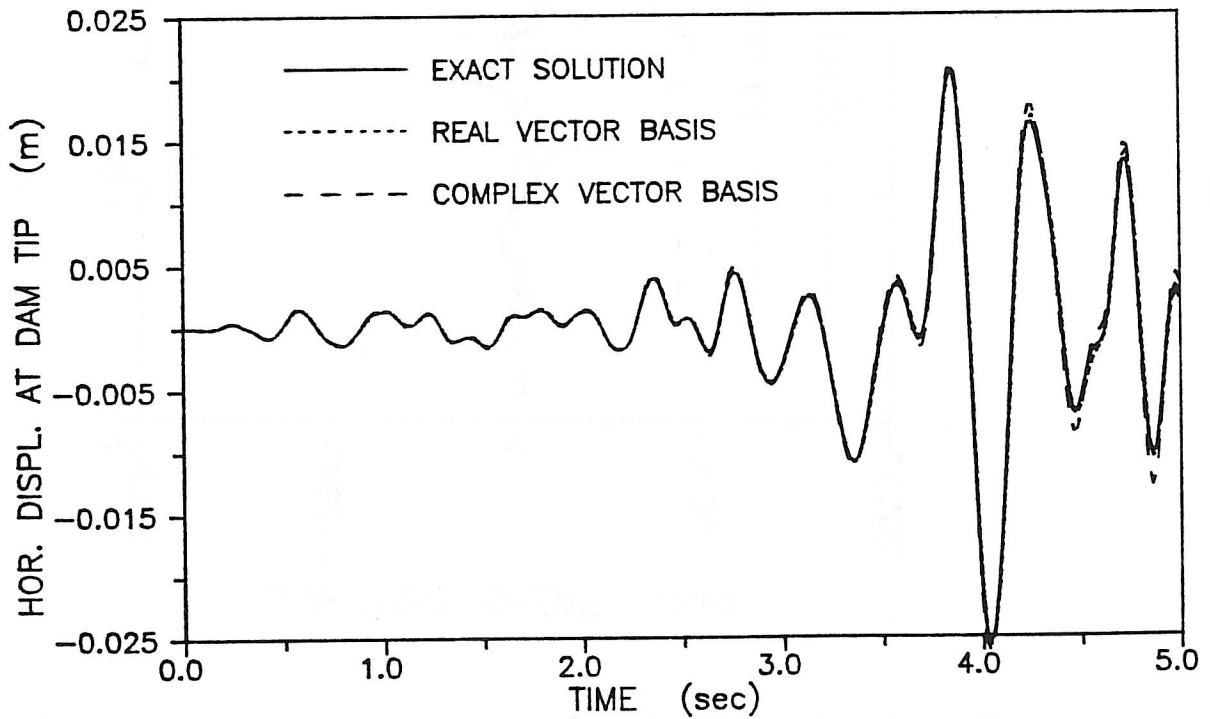


Figure 5.7.b - Horizontal displacement at dam tip for Taft earthquake

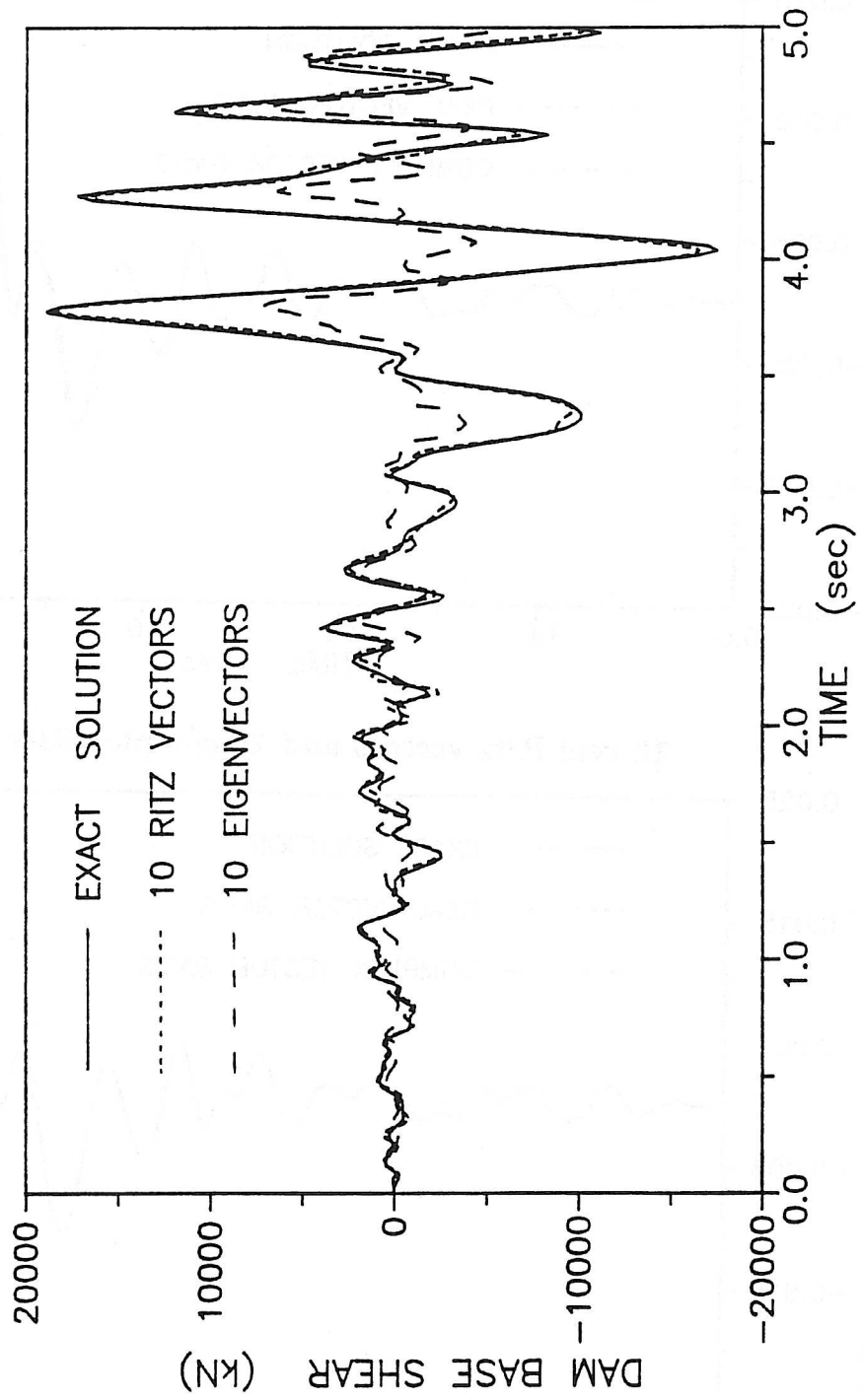


Figure 5.8 - Dam base shear force for eigenvector and Ritz vector basis